

## STEM CELLS AND REGENERATION

## RESEARCH ARTICLE

# Linking the environment, DAF-7/TGF $\beta$ signaling and LAG-2/DSL ligand expression in the germline stem cell niche

Olga Pekar<sup>1</sup>, Maria C. Ow<sup>2</sup>, Kailyn Y. Hui<sup>3</sup>, Marcus B. Noyes<sup>3</sup>, Sarah E. Hall<sup>2</sup> and E. Jane Albert Hubbard<sup>1,\*</sup>

**ABSTRACT**

The developmental accumulation of proliferative germ cells in the *C. elegans* hermaphrodite is sensitive to the organismal environment. Previously, we found that the TGF $\beta$  signaling pathway links the environment and proliferative germ cell accumulation. Neuronal DAF-7/TGF $\beta$  causes a DAF-1/TGF $\beta$ R signaling cascade in the gonadal distal tip cell (DTC), the germline stem cell niche, where it negatively regulates a DAF-3 SMAD and DAF-5 Sno-Ski. LAG-2, a founding DSL ligand family member, is produced in the DTC and activates the GLP-1/Notch receptor on adjacent germ cells to maintain germline stem cell fate. Here, we show that DAF-7/TGF $\beta$  signaling promotes expression of *lag-2* in the DTC in a *daf-3*-dependent manner. Using ChIP and one-hybrid assays, we find evidence for direct interaction between DAF-3 and the *lag-2* promoter. We further identify a 25 bp DAF-3 binding element required for the DTC *lag-2* reporter response to the environment and to DAF-7/TGF $\beta$  signaling. Our results implicate DAF-3 repressor complex activity as a key molecular mechanism whereby the environment influences DSL ligand expression in the niche to modulate developmental expansion of the germline stem cell pool.

**KEY WORDS:** GLP-1/Notch, SMAD, DAF-3, *C. elegans*, Sno-Ski

**INTRODUCTION**

To maintain tissues, stem cells and their dividing progeny are tightly regulated. In addition to direct signals from the stem cell niche, global signals reporting environmental and physiological conditions can influence the outcome of stem cell decisions (Drummond-Barbosa, 2008; Hubbard et al., 2012; Laws and Drummond-Barbosa, 2017). However, our understanding of the mechanisms underlying this regulation remains incomplete.

The *C. elegans* germ line is a powerful model for exploring how stem cell behavior is influenced by the combined action of signaling from the local niche and by organismal cues that report physiologically relevant conditions. In hermaphrodites, a single distal tip cell (DTC) caps each of the two gonad arms and functions as the germline stem cell niche. DTC-to-germline signaling via the Notch pathway and gap junctions governs stem cell fate and proliferation (Kimble and White, 1981; Austin and Kimble, 1987; Starich et al., 2014). At least two of the 10 DSL family ligands in the *C. elegans* genome (Chen and Greenwald, 2004), LAG-2 and APX-1, are produced by the DTC and activate the GLP-1/Notch receptor

on the surface of germ cells to maintain germline stem cell fate (Henderson et al., 1994; Nadarajan et al., 2009). The DAF-7/TGF $\beta$  signaling pathway was identified for its role in dauer formation (Larsen et al., 1995). If animals meet unfavorable conditions as early larvae, the resulting decrease in DAF-7/TGF $\beta$  signaling promotes formation of the stress-resistant, non-aging dauer larva. In this role, DAF-7 signals through the DAF-1 type I and DAF-4 type II receptors and DAF-8 and DAF-14 R-Smads to negatively regulate a DAF-3 SMAD/DAF-5 Sno-Ski transcriptional repressor complex (Gumienny, 2013). We identified the DAF-7/TGF $\beta$  signaling pathway in a genetic screen for genes that modulate the accumulation of proliferative germ cells in later larval stages, after the time that the dauer decision is made (Dalfó et al., 2012). In this role, it uses the same components and regulatory logic as in dauer formation (Fig. 1A), but the DAF-1/TGF $\beta$ R complex and downstream transcriptional regulators act in the DTC (Dalfó et al., 2012). Unlike the DAF-2/insulin-IGF-like signaling pathway that also influences larval germline progenitor cell accumulation (Hubbard et al., 2012; Michaelson et al., 2010), DAF-7/TGF $\beta$  signaling influences germline stem cell fate and not the rate of germ cell cycle progression. Finally, in at least one genetic scenario DAF-7/TGF $\beta$  can act independently of the GLP-1/Notch receptor.

Here, we report that TGF $\beta$  receptor signaling promotes the expression of *lag-2* in the late larval DTC, defining a direct mechanistic link between TGF $\beta$  and Notch signaling. We also extend previous findings on the transcriptional regulation of *lag-2*. We find that DTC expression of *lag-2* is reduced when TGF $\beta$  signaling is low but is restored in the absence of *daf-3* or *daf-5*. Similarly, *lag-2* reporter expression is reduced in unfavorable environments, in a manner dependent on *daf-3*. Using one-hybrid and ChIP assays, we find evidence for direct interaction between DAF-3 and the *lag-2* promoter. Using transcriptional reporters, we define a TGF $\beta$  response element in the *lag-2* promoter and show that eliminating one of two potential DAF-3-binding sites abrogates the response to TGF $\beta$  receptor signaling and to low food, suggesting that it may serve as a direct target for the TGF $\beta$  pathway within the *lag-2* promoter. We propose a working model and discuss our findings in the context of previous work, of TGF $\beta$ -Notch and environment-Notch interactions in general.

**RESULTS****DAF-7/TGF $\beta$  signaling promotes *lag-2* expression**

We sought to determine the mechanistic link between TGF $\beta$ R signaling in the DTC and germline stem cell maintenance. Previously, we showed that TGF $\beta$ R signaling in the DTC promotes germ cell accumulation during late larval stages by preventing germ cell differentiation. Our previous work suggested that the TGF $\beta$ R can act in parallel to GLP-1/Notch (Dalfó et al., 2012). This conclusion was based on: (1) the observation that reducing TGF $\beta$  signaling in a *glp-1*(null) mutant, which was also mutant for *gld-1* and *gld-2*, to permit production and maintenance of

<sup>1</sup>Skirball Institute of Biomolecular Medicine and Department of Cell Biology, NYU School of Medicine, New York, NY 10016, USA. <sup>2</sup>Department of Biology, Syracuse University, Syracuse, NY 13244, USA. <sup>3</sup>Institute for Systems Genetics, NYU School of Medicine, New York, NY 10016, USA.

\*Author for correspondence (jane.hubbard@med.nyu.edu)

✉ E.J.A.H., 0000-0001-5893-7232

Received 6 December 2016; Accepted 1 July 2017

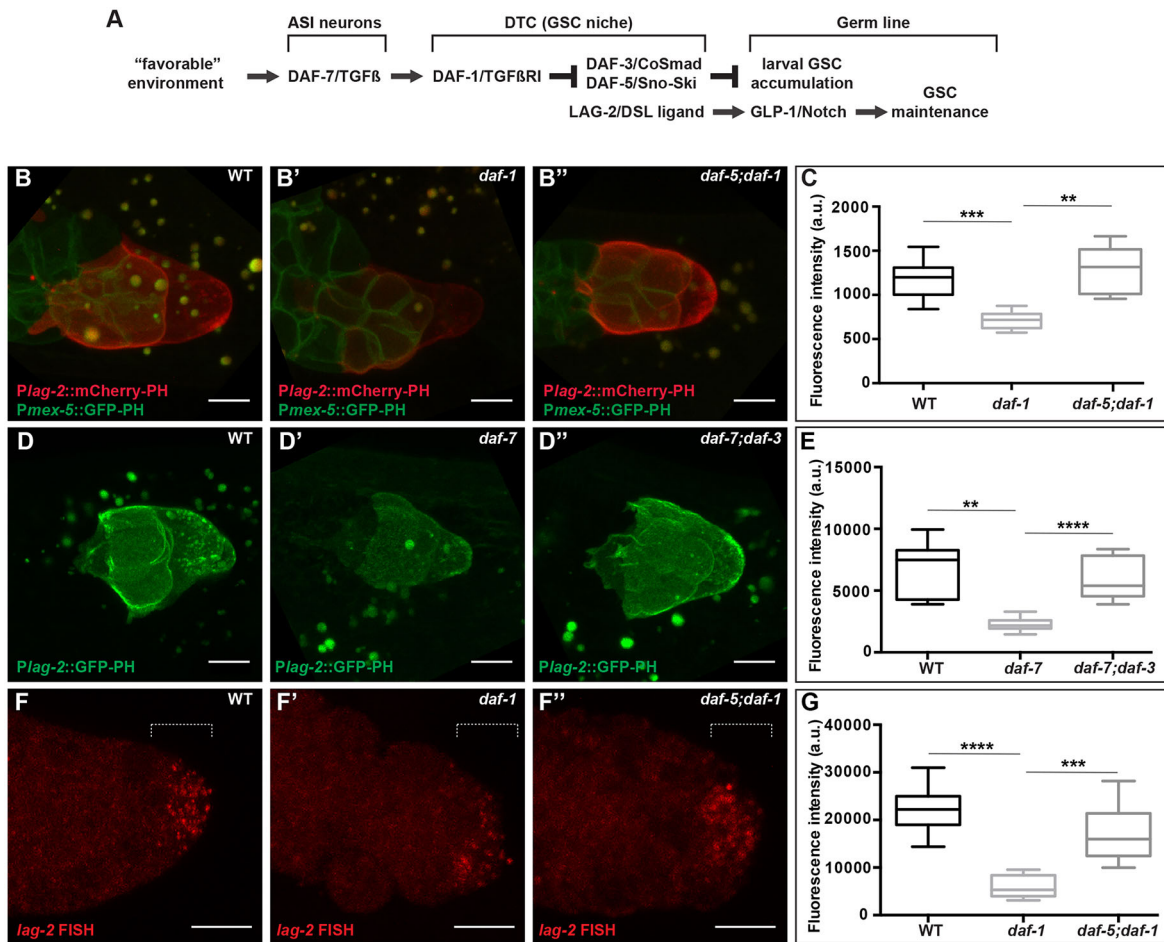


**Fig. 1.** DAF-7/TGF $\beta$  signaling promotes *lag-2* expression in the DTC. (A) Summary of the influences of larval DAF-7/TGF $\beta$  and GLP-1/Notch signaling reported prior to this work. (B–E) Expression of *lag-2* (3 kb upstream) reporters. *nals37*: membrane-bound mCherry (mCherry-PH) low-copy reporter in the distal gonad arm of (B) wild-type, (B') *daf-1* and (B'') *daf-5;daf-1* animals. *naS11* [*Pmex-5::GFP-PH*] marks germ cell membranes. See Fig. S1 for additional genotypes. *naS18*: membrane-bound GFP (GFP-PH) single-copy reporter in (D) wild-type, (D') *daf-7* and (D'') *daf-7;daf-3* animals. (C,E) Quantification of mCherry and GFP signals, respectively. (F–G) *In situ* hybridization with *lag-2* probes of dissected gonads from (F) wild-type, (F') *daf-1* and (F'') *daf-5;daf-1* animals (magnified relative to other panels). (C,E,G) Values correspond to mean pixel intensity (C,E) and sum pixel intensity (G) in arbitrary units, measured in the DTC as described in the Materials and Methods. The boxes indicate the minimum–maximum range of samples quantified. Dotted lines mark the area (distal 5  $\mu$ m) where the signal was quantified in G. This signal is in the DTC, not in the germ line. Scale bars: 5  $\mu$ m. Mutant alleles: *daf-1(m40)*, *daf-5(e1386)*, *daf-7(e1372)* and *daf-3(e1376)*. \*\*P<0.01, \*\*\*P<0.001, \*\*\*\*P<0.0001, two-tailed Student's t-test. n≥15 animals, one DTC scored per animal. Error bars represent s.e.m. In all cases, P>0.05 for wild type versus double mutants.

proliferative germ cells, reduced the number of germ cells in the resulting germline tumors; and (2) our inability to detect consistent changes in then-existing *lag-2* reporter expression upon manipulation of the TGF $\beta$  pathway (Dalfó et al., 2012; E.J.A.H., unpublished). Although the residual effects of TGF $\beta$  signaling in the *glp-1(null)* mutant (albeit tumorous) background still argue for a partially GLP-1-independent role for TGF $\beta$  signaling (see Discussion), results presented here suggest that TGF $\beta$  signaling also influences GLP-1 activity by modulating expression of a DSL ligand, LAG-2, in the DTC.

Given our provisional conclusion that GLP-1/Notch was not acting downstream of TGF $\beta$ , we set out to investigate the possibility that the DTC-germline interface might be disrupted when TGF $\beta$  signaling was low. We built DTC membrane-bound reporters (using GFP or mCherry fusions to the PH domain of the rat PLC181) driven by the 3 kb *lag-2* upstream region used by others (Henderson et al., 1994). We introduced the new reporter transgenes into the worm genome using microparticle bombardment, a technique that results in fewer copies than traditional transgenes borne on

extrachromosomal arrays. We examined the DTC in the fourth larval stage (L4) as DAF-7/TGF $\beta$  signaling affects proliferative germ cell accumulation before and during this stage (Dalfó et al., 2012). We observed that the reporters were expressed at an overall lower level in wild type than reporters we had examined previously.

To our surprise, the new lower-copy reporters were expressed at significantly lower levels in *daf-7* or *daf-1* mutant backgrounds than in the wild type, and their expression was restored to wild-type levels in *daf-7* or *daf-1* double mutants with *daf-3* or *daf-5* (Fig. 1B,C, Fig. S1A–C). The restoration of expression in these double mutants is consistent with the logic of the canonical DAF-7/TGF $\beta$  pathway that we previously implicated in the regulation of the germline proliferative pool (Fig. 1A). Similar effects were observed with a single-copy reporter introduced by MosSCI (Fig. 1D,E) and with either mCherry or GFP reporters. A different non-*lag-2* DTC-expressed reporter showed no such regulation (Fig. S1D,E). Therefore, we conclude that the lower copy number and expression levels of the newer reporters reveals modulation by the DAF-7/TGF $\beta$  pathway that was not detectable with high-copy reporters.

To determine whether the reporters were reflecting changes in endogenous *lag-2* mRNA in the DTC, we performed fluorescence *in situ* hybridization experiments on dissected gonad preparations. Our results were consistent with the reporter analysis (Fig. 1F,G), suggesting that *lag-2* expression in the DTC is regulated positively by DAF-7/TGF $\beta$  signaling and negatively by DAF-3 and DAF-5.

### **Environmental conditions alter *lag-2* expression, dependent on the DAF-7/TGF $\beta$ signaling pathway**

Previously, we showed that DAF-7/TGF $\beta$  signaling regulates the accumulation of proliferative zone cells in the larval germ line in response to low food or high dauer pheromone, two conditions that reduce *daf-7* expression in ASI neurons (Ren et al., 1996; Schackwitz et al., 1996). To determine whether *lag-2* expression is similarly modulated, we measured GFP expression from a single-copy *lag-2* reporter under favorable (high food or low pheromone) and unfavorable (low food or high pheromone) conditions (Fig. 2). We found that *lag-2* reporter expression was diminished in either unfavorable condition relative to the favorable condition in the wild type (Fig. 2B,F). The *daf-7* mutant displayed lower expression that was not further reduced by unfavorable conditions (Fig. 2B',F'). In the *daf-7; daf-3* double mutant, *lag-2* reporter expression is restored to that of favorable conditions in the wild type, even under unfavorable conditions (Fig. 2B'',F''). These results suggest that environmental regulation of *lag-2* expression occurs through the canonical DAF-7/TGF $\beta$  pathway. Consistent with previous results (Dalfó et al., 2012), germ cell accumulation in all these environmental and genetic combinations parallels observed changes in *lag-2* reporter expression (Fig. 2).

### **Canonical DAF-3 SMAD-binding sites in the *lag-2* promoter do not mediate DAF-7/TGF $\beta$ signaling in the DTC**

We hypothesized that *lag-2* expression may be negatively regulated by the DAF-3 repressor complex through direct interaction with *lag-2* regulatory sequences. Within the 3 kb region upstream of *lag-2*, we found three instances of the 5 bp DAF-3 binding motif (Fig. 3A) previously defined in the *myo-2* promoter (Thatcher et al., 1999), and that are also present within a DAF-3-bound region in the promoters of *daf-7* and *daf-8*, as determined by whole-animal ChIP (Park et al., 2010). If these sites mediate DAF-3 repressor activity, mutating them should render *lag-2* expression insensitive to the loss of *daf-7* or *daf-1*. We generated two independent lines, one bearing a promoter with all three sites mutated that drives mCherry and the other bearing the wild-type promoter that drives GFP (Fig. 3A). We crossed them to generate a strain bearing both reporters and assessed their expression in the wild type and *daf-7* mutant. As expected, we observed lower wild-type promoter ('wt *lag-2* promoter', green in Fig. 3B) expression in the *daf-7* mutant background. However, we also observed lower expression from the mutant promoter in *daf-7* relative to wild type (Fig. 3B,C). The differences in mutant promoter-driven expression were also apparent in strains without the wild-type GFP reporter (data not shown). These results suggest that the predicted canonical DAF-3-binding sites do not confer regulation of *lag-2* expression by the DAF-7/TGF $\beta$  pathway in this context.

### **An ~100 bp sequence upstream of *lag-2* is required for the response to DAF-7/TGF $\beta$ signaling**

To identify the TGF $\beta$ -responsive region of the *lag-2* promoter, we performed promoter deletion analysis. We generated strains expressing reporters of 2.0, 1.0 and 0.5 kb upstream of the ATG. We then crossed the transgenes into *daf-7* and *daf-7; daf-3* mutant backgrounds and compared their expression (Fig. 4). Consistent

with previous reports of *lag-2* expression in head neurons (Ouellet et al., 2008; Singh et al., 2011), our 1.0 kb promoter drove reporter expression in head neurons, as well as in the DTC. This expression in neurons was not grossly affected by DAF-7/TGF $\beta$  pathway signaling and served as an internal control (Fig. S2). Each of the three promoter regions tested showed reduced expression in the *daf-7* single mutant that was restored to wild-type levels in *daf-7; daf-3* double mutants (Fig. 4A-F). We next assessed a promoter truncated at -405 bp. This reporter no longer responded to the loss of *daf-7*: expression was similar in wild type, *daf-7* and *daf-7; daf-3*. Taken together, these results define a key TGF $\beta$ -responsive element (TRE) near or within the -405 to -500 region upstream of *lag-2* (Fig. 4G,H).

### **A 25 bp sequence mediates the *lag-2* promoter response to TGF $\beta$ signaling and the environment**

Closer inspection of the TRE upstream of *lag-2* revealed homology to a *cis*-acting regulatory sequence named the PD motif, which was characterized in the *osm-9* promoter in the context of continuous versus postdauer (PD) development (Sims et al., 2016). The *osm-9* PD motif consists of two sequence elements: a DAF-3-binding site (*osm-9p-DBS*) and a conserved sequence (*osm-9p-Cons*) that is found in the upstream regulatory regions of ~1000 genes of the *C. elegans* genome (Sims et al., 2016). At the *lag-2* locus, we identified an 8 bp sequence with homology to the *osm-9* promoter that partially overlaps with the *osm-9p-DBS* at -577 to -570 upstream of the *lag-2* ATG (*lag-2p-DBS*). Whereas the *osm-9p-DBS* contains a canonical SMAD-binding sequence (GTCT), the *lag-2p-DBS* does not (Fig. S3). In addition, we identified a 25 bp loosely conserved sequence from -432 to -407 (*lag-2p-Cons*) that, although not identical to the *osm-9p-Cons*, satisfies much of the conserved (Cons) sequence 'rule' (Fig. S3). The *lag-2p-DBS* sequence is upstream of the TRE, and the *lag-2p-Cons* is within the TRE that we defined by promoter deletion analysis (Fig. 5A). We generated reporter strains with each site deleted individually or together in the context of the 1 kb *lag-2* upstream fragment (Fig. 5B-G). Expression of the reporter lacking the *lag-2p-DBS* sequence was still reduced in *daf-7* relative to wild type, albeit not as much as when the sequence was intact (Fig. 5B,C). By contrast, the reporter lacking the *lag-2p-Cons* motif was expressed at the same level in the wild type and in the *daf-7* mutant (Fig. 5D,E). These results indicate that the 25 bp *lag-2p-Cons* sequence is required for the TGF $\beta$  response in the L4 DTC.

To determine whether *lag-2* reporter expression in response to the environment (Fig. 2) is similarly regulated by the Cons sequence, we repeated the low-food experiment in strains bearing the 1 kb *lag-2* upstream fragment with and without the Cons sequence. We measured expression of GFP in the DTC of L4 animals raised on low or high bacterial concentration and, as a positive control for the effects of low food, measured the number of proliferative germ cells. We observed that in the absence of the Cons sequence, the reporter was no longer sensitive to the food level (Fig. S4), suggesting that the Cons sequence mediates the *daf-3*-dependent effect of low food on *lag-2* expression.

### **DAF-3 binds upstream of *lag-2***

In the *osm-9* promoter, DAF-3 SMAD is enriched at the *osm-9p-DBS* within the PD motif to downregulate *osm-9* in ADL neurons of animals that passed through the dauer stage (Sims et al., 2016). To determine whether DAF-3 is enriched at the PD motif elements upstream of *lag-2*, we performed DAF-3 immunoprecipitation on whole worms using a commercially available antibody followed by quantitative PCR of the *lag-2* upstream sequences in the wild type

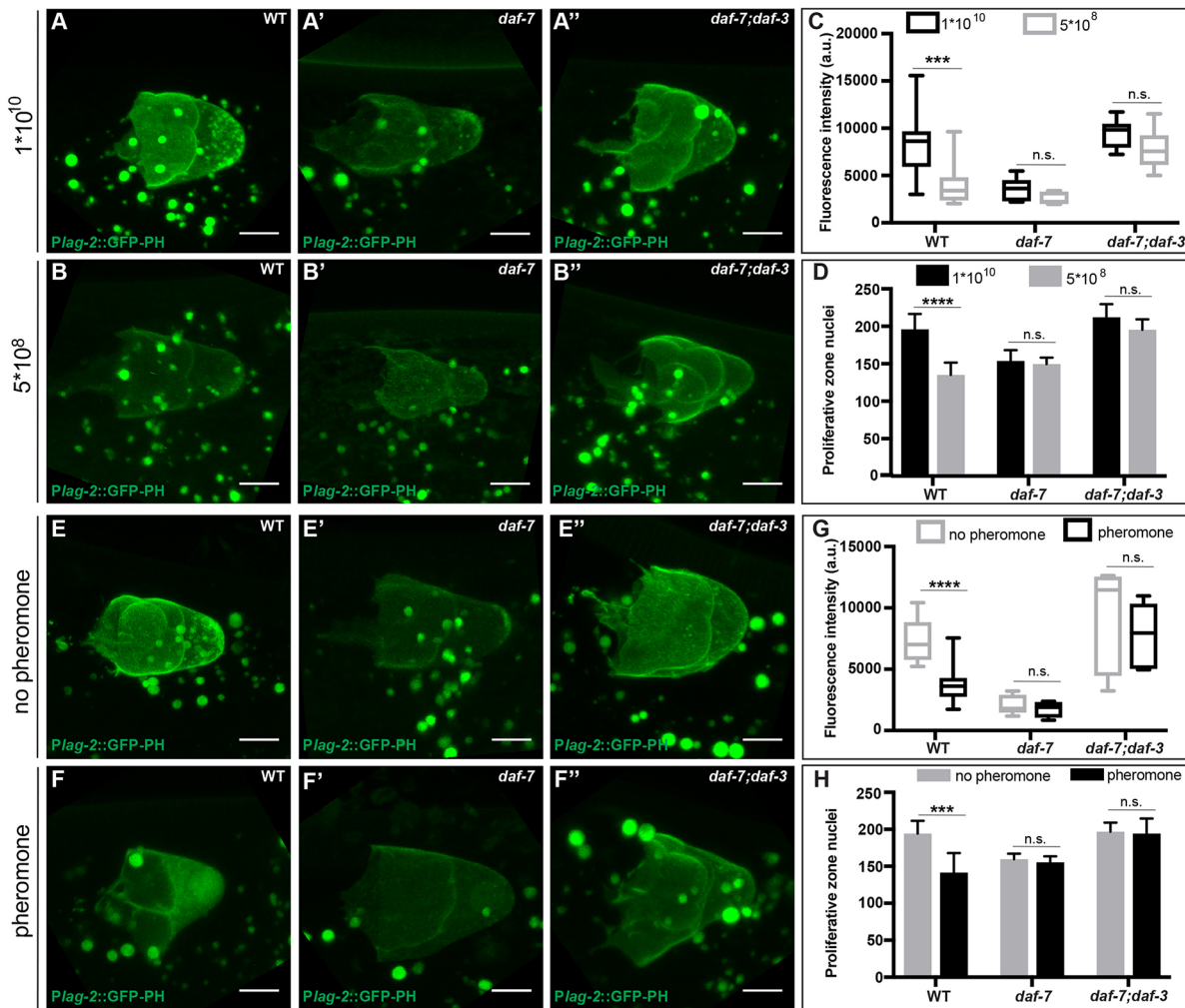


**Fig. 2. Reduced *lag-2* DTC expression under adverse environmental conditions depends on *daf-3*.** (A–B'') Expression levels of the *lag-2* single-copy reporter *naS8* in the DTC of late L4 animals reared from early L3 on a high ( $1 \times 10^{10}$ ) or low ( $5 \times 10^8$ ) concentration of OP50 bacteria in (A,B) wild-type, (A',B') *daf-7* and (A'',B'') *daf-7;daf-3* animals. (C) Quantification of the GFP signal in the DTC in animals exposed to high or low bacterial concentrations. (D) Number of proliferative zone nuclei per gonad arm in early adults (collected from the same plates as in previous panels) reared from early L3 under high or low bacterial concentrations. (E–F'') Expression levels of *lag-2* single-copy reporter (*naS8*) in the DTC of late L4 animals in the absence or presence of exogenous dauer pheromone introduced in the early L3 in (E,F) wild-type, (E',F') *daf-7* and (E'',F'') *daf-7;daf-3* animals. A slight enrichment of nuclear GFP was observed under high-pheromone conditions (but not under low-food conditions) in a majority of animals, but its significance was not further investigated. (G) Quantification of the GFP signal in the DTC in animals exposed or not exposed to exogenous dauer pheromone. (C,G) Mean pixel intensity (arbitrary units), measured in the DTC as described in the Materials and Methods. The boxes indicate the minimum-maximum range of samples quantified. (H) Number of proliferative zone nuclei of early adults (collected from the same plates as in previous panels) exposed or not exposed to exogenous dauer pheromone introduced in the early L3 stage. Scale bars: 5  $\mu$ m. Mutant alleles were *daf-7(e1372)* and *daf-3(e1376)*. n.s. indicates  $P > 0.05$ , \*\*\* $P < 0.001$ , \*\*\*\* $P < 0.0001$ , two-tailed Student's *t*-test.  $n \geq 15$  animals, one DTC scored per animal (GFP quantifications) or one gonadal arm per animal (proliferative zone quantifications). Error bars represent s.e.m. Additional statistical analysis in GFP quantifications:  $P > 0.05$  for the wild type under high-food or no pheromone conditions versus *daf-7;daf-3* double mutant under low-food or with pheromone conditions, respectively.

and the *daf-3(mgDf90)* mutant. Our results indicate that DAF-3 is significantly enriched at the *lag-2*p-DBS in wild-type L4 animals compared with background levels of enrichment in the *daf-3(mgDf90)* strain (Fig. 6A). As expected, DAF-3 was not enriched at the *osm-9*p-DBS in larval L4 animals that experienced continuous (non-dauer) development (Sims et al., 2016). Interestingly, we found that DAF-3 was enriched at the Cons sequences in both *lag-2* (*lag-2*p-Cons) and *osm-9* (*osm-9*p-Cons), suggesting that binding may occur at multiple sites within the PD motif (Fig. S5A). As positive controls, we verified DAF-3 enrichment at its characterized binding sites in the *myo-2*, *daf-7* and *daf-8* promoters (Park et al., 2010; Thatcher et al., 1999). Furthermore, DAF-3 was not enriched in the *lag-2*-coding region, similar to our negative control, *daf-14*

(Fig. S5A) (Park et al., 2010). Together, these results indicate that the *lag-2* upstream regulatory region contains the *lag-2*p-DBS and *lag-2*p-Cons sequence components of the PD motif, both of which have enriched DAF-3 binding in the ChIP assay.

#### One-hybrid studies support direct binding of DAF-3 to both PD motif elements within the *lag-2* upstream region

We sought independent evidence for binding of DAF-3 to the *lag-2* promoter. We turned to a bacterial one-hybrid approach that has advantages of high sensitivity and quantifiable results (Noyes, 2012). We found that the N-terminal DNA-binding region of DAF-3 showed greater binding in the presence of the 600 bp sequence upstream of the *lag-2* ATG (Fig. 6B, Fig. S5B). To assess

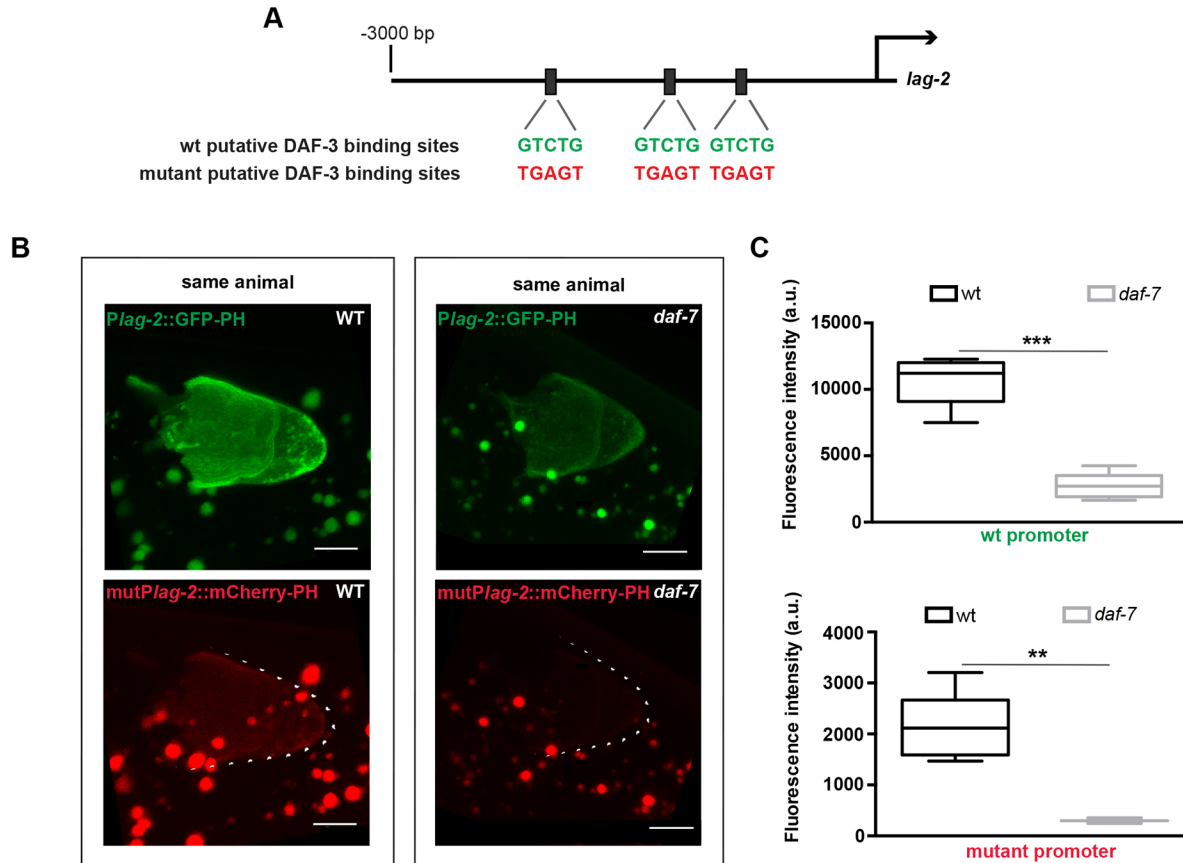


**Fig. 3. Canonical DAF-3-binding sites are not required for the effect of DAF-7/TGF $\beta$  on *lag-2* DTC expression.** (A) Positions of three canonical DAF-3-binding sites (Thatcher et al., 1999) within 3 kb upstream of the *lag-2* ATG. (B) Distal gonad arms from two animals, each expressing two reporters: the wild-type single-copy *naS18* GFP-PH reporter; and *nals96*, an integrated reporter in which mCherry-PH is driven by a *lag-2* promoter, in which three canonical DAF-3-binding sites were mutated as in A. The expression of each reporter was measured in individual wild-type (left) and *daf-7*(e1372) (right) animals. Scale bars: 5  $\mu$ m. (C) Quantification of GFP (top) and mCherry (bottom) in the DTC in the different genetic backgrounds. Mean pixel intensity (arbitrary units), measured in the DTC as described in the Materials and Methods. The boxes indicate the minimum-maximum range of samples quantified. \*\*P<0.01, \*\*\*P<0.001, two-tailed Student's t-test. n≥15 animals, one DTC scored per animal. Error bars represent s.e.m.

the relevance of the PD motif in this binding assay, we deleted or scrambled the *lag-2*p-DBS and *lag-2*p-Cons sequences individually and in tandem. We found that deleting either site lowered binding (Fig. 6B). Although scrambling only one sequence had no effect, scrambling both significantly reduced binding (Fig. S5B). We conclude that, although the Cons site alone is required to regulate DTC reporter expression, binding can occur at either site, consistent with the whole-worm ChIP-qPCR analysis.

## DISCUSSION

Our results indicate that the environment impacts the expression of a DSL ligand, *lag-2*, in the germline stem cell niche through TGF $\beta$  signaling. When conditions are poor (low food or high pheromone), *lag-2* reporter expression is reduced, and this reduction is dependent on DAF-3 SMAD activity. Furthermore, this reduction is dependent on a 25 bp conserved (Cons) region of the *lag-2* promoter (Fig. S4). Together with our previous studies (Dalfó et al., 2012), this work suggests a simple working model (Fig. 7) in which proliferative germ cells accumulate in favorable conditions in response to DAF-7/TGF $\beta$  signaling that ensures high levels of LAG-2 in the DTC, that then signals to GLP-1/Notch in the germ line. That DAF-7/TGF $\beta$  signaling may modulate Notch activity is consistent with previous results showing that low *daf-1* activity enhances the phenotype of a *glp-1* reduction-of-function mutant and that, similar

to *glp-1*, *daf-1* does not affect the mitotic index of the proliferative pool (Dalfó et al., 2012).

Our current results show that DAF-3 SMAD can bind both the DBS and the Cons sequences in the *lag-2* promoter in the L4 (in whole-worm ChIP), even when conditions are favorable and animals have experienced continuous development. Work by others has shown that DAF-3 can also bind to *mdl-1*, *daf-7* and *daf-8* promoters in non-dauer animals (Deplancke et al., 2006; Park et al., 2010), and Sims et al. (2016) demonstrated that DAF-3 bound the *osm-9* promoter in continuously developing adult animals, which was dependent upon functional ZFP-1/AF10 protein and endogenous RNAi pathways. Spacing may also be important for DAF-3 binding of DBS and Cons, as binding in the bacterial one-hybrid assay was maintained when the sites were individually scrambled (rather than deleted) but was lost when both were scrambled (Fig. S5B). Subcellular localization of DAF-3 is not grossly altered by changes in TGF $\beta$  signaling (Patterson et al., 1997). Thus, DAF-3 activity as a transcriptional repressor may not correlate solely with its ability to bind DNA. For example, it could depend on post-translational modifications or additional DNA-binding partners. In unfavorable conditions when TGF $\beta$  receptor signaling is low, we speculate that the DAF-3 repressor complex at the Cons sequence becomes active in the DTC (Fig. 7).

How does the DAF-3 repressor complex repress transcription? Among many possible mechanisms, the active repressor complex

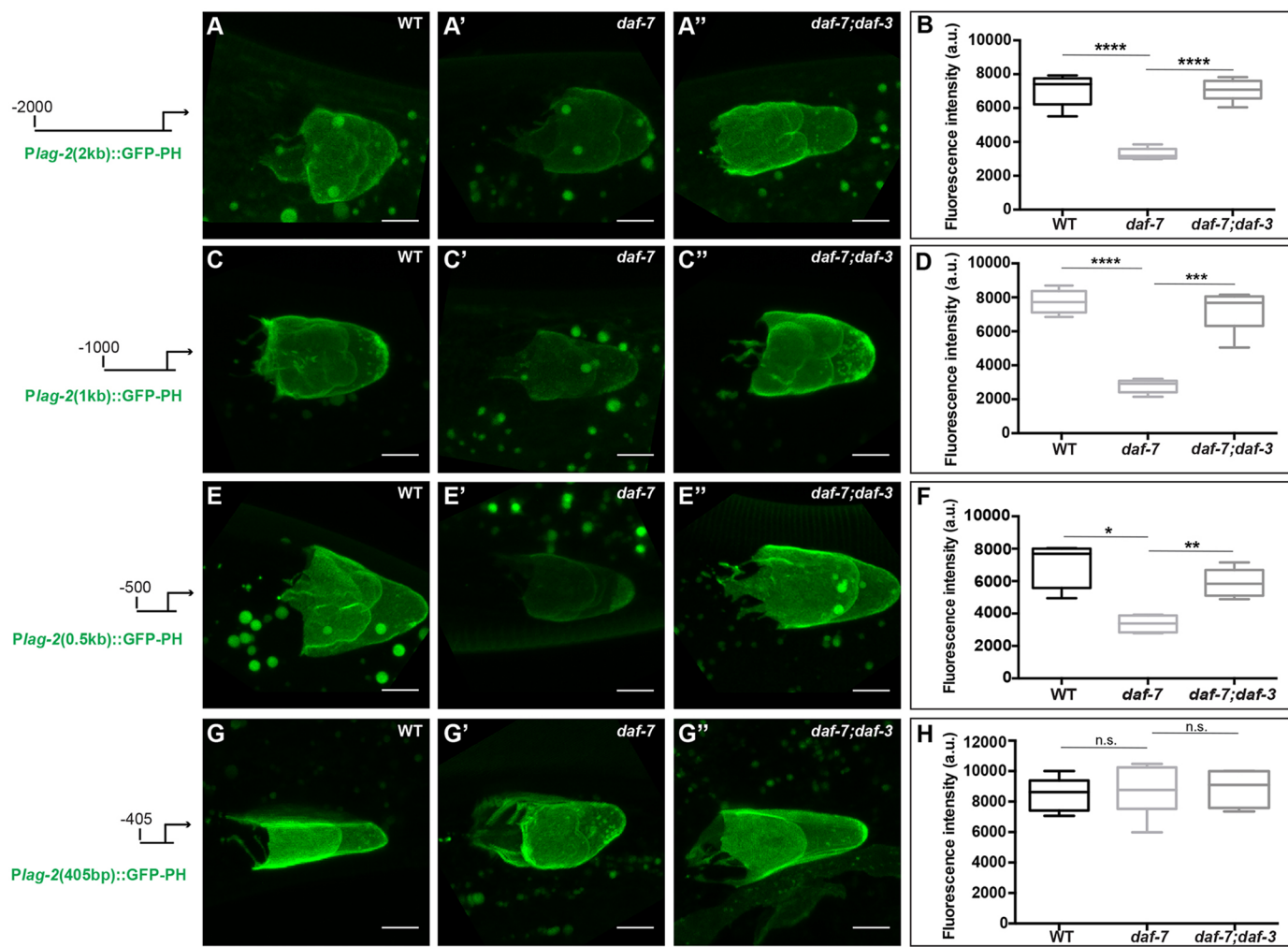


**Fig. 4. A region between  $-500$  bp and  $-405$  bp in the *lag-2* promoter is crucial for the DTC response to DAF-7/TGF $\beta$ .** Expression levels of *lag-2* low-copy GFP-PH reporters driven by (A-B) 2 kb, (C-D) 1 kb, (E-F) 500 bp and (G-H) 405 bp upstream in the DTC of wild-type, *daf-7(e1372)* and *daf-3(e1376)* animals. Transgene alleles are *nals81*, *nals84*, *nals87* and *nals98*, respectively. (B,D,F,H) Mean pixel intensity (arbitrary units), measured in the DTC as described in the Materials and Methods. The boxes indicate the minimum-maximum range of samples quantified. Scale bars: 5  $\mu$ m. n.s. indicates  $P>0.05$ , \* $P<0.05$ , \*\* $P<0.01$ , \*\*\* $P<0.001$ , \*\*\*\* $P<0.0001$ , two-tailed Student's *t*-test.  $n\geq 15$  animals, one DTC scored per animal. Error bars represent s.e.m. In all cases,  $P>0.05$  for wild type versus double mutants.

may interfere with activators at nearby sites. The helix-loop-helix (HLH) transcription factor HLH-2/Da activates *lag-2* via enhancer box (E-box) sequences (Krause et al., 1997) that are close to the Cons sequence. However, we found that the active DAF-3 complex is unlikely to interfere with HLH-2, because depleting *hh-2* by RNAi reduced *lag-2* reporter expression in wild-type, *daf-7* and *daf-7;daf-3* (Fig. S6 and supplementary Materials and Methods for RNAi methods). Interfering with *hh-2* or E-boxes reduces but does not eliminate DTC *lag-2* expression, suggesting that other transcription factors contribute (Chesney et al., 2009; Karp, 2003; Karp and Greenwald, 2004). We found highly conserved sequences within 500 bp upstream of the ATG: a GC-box, a C/EBP box and an uncharacterized sequence (Fig. S7). Deletion of any one of these sites abrogated reporter expression (data not shown). Therefore, the DAF-3 repressor complex may interfere with activators that bind these sites.

If modulation of DTC *lag-2* expression and its subsequent effects on germline GLP-1/Notch receptor activity were the only mechanism by which the larval germ line responds to DAF-7/TGF $\beta$ , the germline progenitor pool should be insensitive to TGF $\beta$  in the absence of *glp-1*. However, we previously showed that fewer germline progenitor cells accumulate when DAF-7/TGF $\beta$  signaling

is low, even in the absence of the GLP-1/Notch receptor, albeit in a tumorous germline context (Dalfó et al., 2012). These results suggest a *glp-1*-independent role for TGF $\beta$ . One possibility is that the other Notch receptor in the *C. elegans* genome, LIN-12, has a partially redundant germline-autonomous role in maintaining germline stem cells. Null mutations in *lin-12* cause sterility, likely secondary to its roles in the somatic gonad (Greenwald et al., 1983; Seydoux et al., 1990), and no obvious larval germline *lin-12* expression is detected by *in situ* hybridization (NEXTDB; Shin-i and Kohara, 1999). We found that *lin-12* RNAi directed primarily to the germ line (in *rrf-1*; Sijen et al., 2001) did not impact the size of the proliferative pool in *glp-1(+)* or *glp-1(rf)*, a highly sensitized background for germline stem cell loss (Fig. S8; see supplementary Materials and Methods for RNAi methods). Additional models include a Notch signaling-independent role for DTC *lag-2* or a *lag-2*-independent role for TGF $\beta$ . For example, TGF $\beta$  signaling may influence DTC-germline gap junctions that promote proliferation (Starich et al., 2014). Unlike the well-characterized role for TGF $\beta$  in the non-tumorous scenario, it is unknown whether the *glp-1*-independent effect of TGF $\beta$  on tumor cell number is DTC autonomous or *daf-3* dependent. In any case,

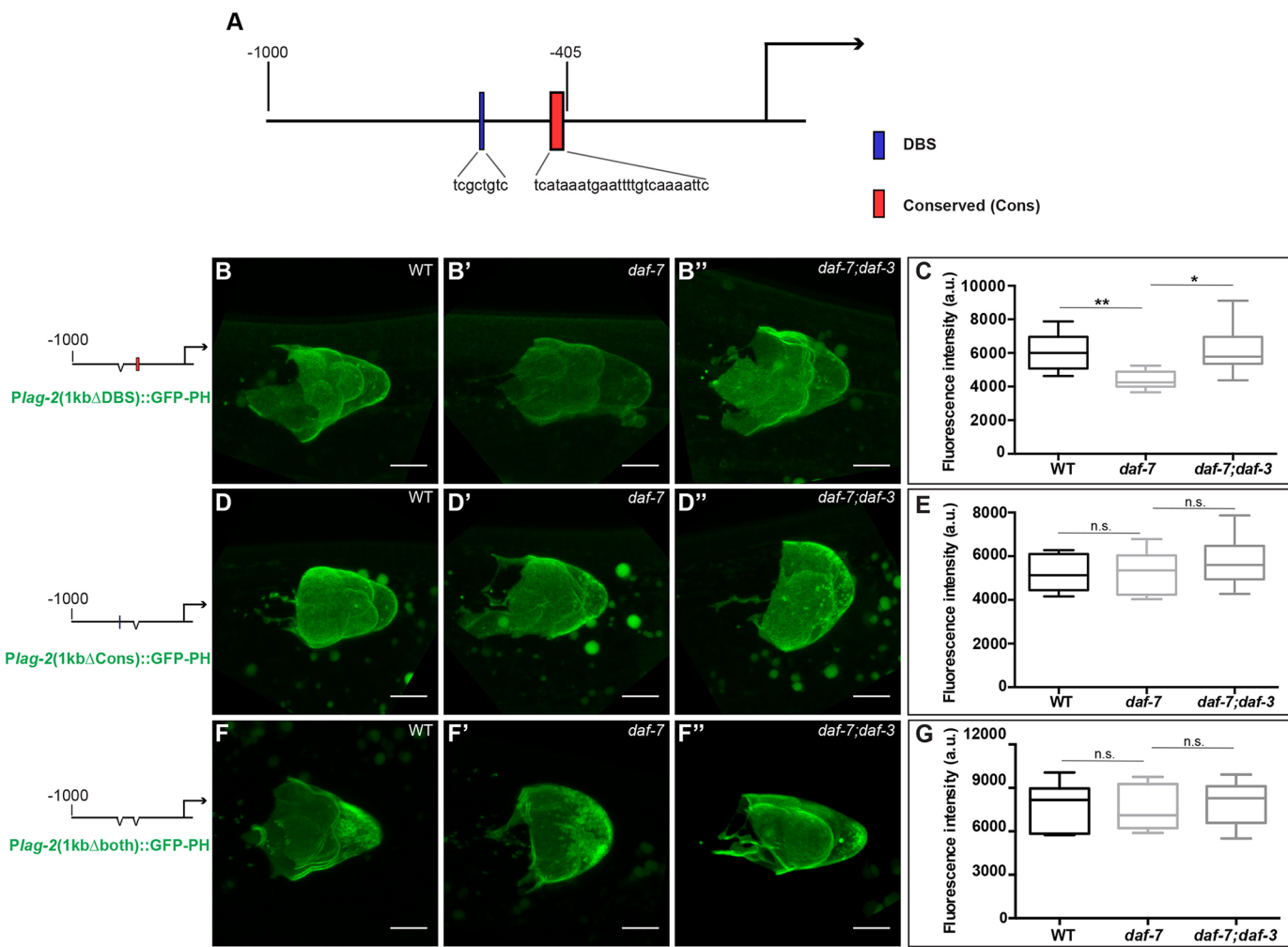


**Fig. 5. The conserved (Cons) sequence is required for the response of *lag-2* to DAF-7/TGF $\beta$  signaling in the DTC.** (A) Positions of the DAF-3-binding site (DBS) and conserved (Cons) sequences. (B–G) Expression of *lag-2* (1 kb, low-copy) GFP-PH reporters in the DTC of wild-type, *daf-7(e1372)* and *daf-7(e1372);daf-3(e1376)* animals. Reporters are lacking (B–C) DBS sequence (1kb $\Delta$ DBS), *nals100*; (D–E) conserved (Cons) sequence (1kb $\Delta$ Cons), *nals102*; or both (F–G), *nals106*. (C,E,G) Quantification of GFP expression; mean pixel intensity (arbitrary units), measured in the DTC as described in Materials and Methods. The boxes indicate the minimum–maximum range of samples quantified. Scale bars: 5  $\mu$ m. n.s. indicates  $P>0.05$ , \* $P<0.05$ , \*\* $P<0.01$ , two-tailed Student's *t*-test.  $n\geq 15$  animals, one DTC scored per animal. Error bars represent s.e.m. In all cases,  $P>0.05$  for wild type versus double mutants.

we propose that TGF $\beta$  regulation of DTC *lag-2* expression reported here accounts for much of the germ cell fate regulation by TGF $\beta$  in the presence of *glp-1*.

In apparent conflict with our results, and as noted by Dalfó et al., (2012), Park et al. (2010) reported that *daf-8*/R-Smad negatively regulates *lag-2* high-copy reporter expression in the DTC and germline proliferative zone size, independently of *daf-3*. Dalfó et al. (2012) observed positive regulation (i.e. less accumulation of proliferative germ cells in *daf-7*, *daf-1*, *daf-8* and *daf-14* mutants), dependent on *daf-3* and *daf-5*. Here, consistent with Dalfó et al., (2012) we show that DAF-7/TGF $\beta$  signaling promotes late larval *lag-2* expression and proliferative germ cell accumulation in a *daf-3*- and *daf-5*-dependent manner. A major difference in the two studies is that Park et al. (2010) focused on adults, whereas we focused on synchronized late larval stages. It remains possible that DAF-8 plays opposite roles in DTC *lag-2* regulation at different life stages. We also observed that the DBS and Cons sites may mediate activation (rather than repression) of a *lag-2* reporter in neurons, indicating cell-specific regulatory differences (data not shown). Consistent with Park et al. (2010), we found enrichment of DAF-3 at the *daf-7* and *daf-8* promoters using whole-worm ChIP (Fig. S5A). A more

complete understanding awaits additional comparative studies of all pathway components in specific cell types at different stages in tightly synchronized animals reared in well-controlled environments.

#### TGF $\beta$ -mediated regulation of DSL ligands and Notch signalling in other systems

Examples of DSL ligand regulation by TGF $\beta$  superfamily members exist in several systems. This may reflect an ancient relationship between these signaling pathways that, together with Wnt, existed in the earliest metazoans (Richards and Degnan, 2010). Examples of positive regulation include TGF $\beta$  promoting *Jag1* expression or activity in the epithelial-to-mesenchymal transition in mammalian cell lines (Zavadil et al., 2004), muscle differentiation of mesenchymal stem cells (Kurpinski et al., 2010), and an endothelial-to-hematopoietic transition in zebrafish (Monteiro et al., 2016). Positive regulation also occurs in endothelial cell lines where a Smad1/5-binding motif was identified upstream of *Jag1* by ChIP-seq (Morikawa et al., 2011). Nodal also positively regulates *Ci-Delta2* transcription in notochord specification in *Ciona* (Hudson and Yasuo, 2005, 2006). It will be of interest to

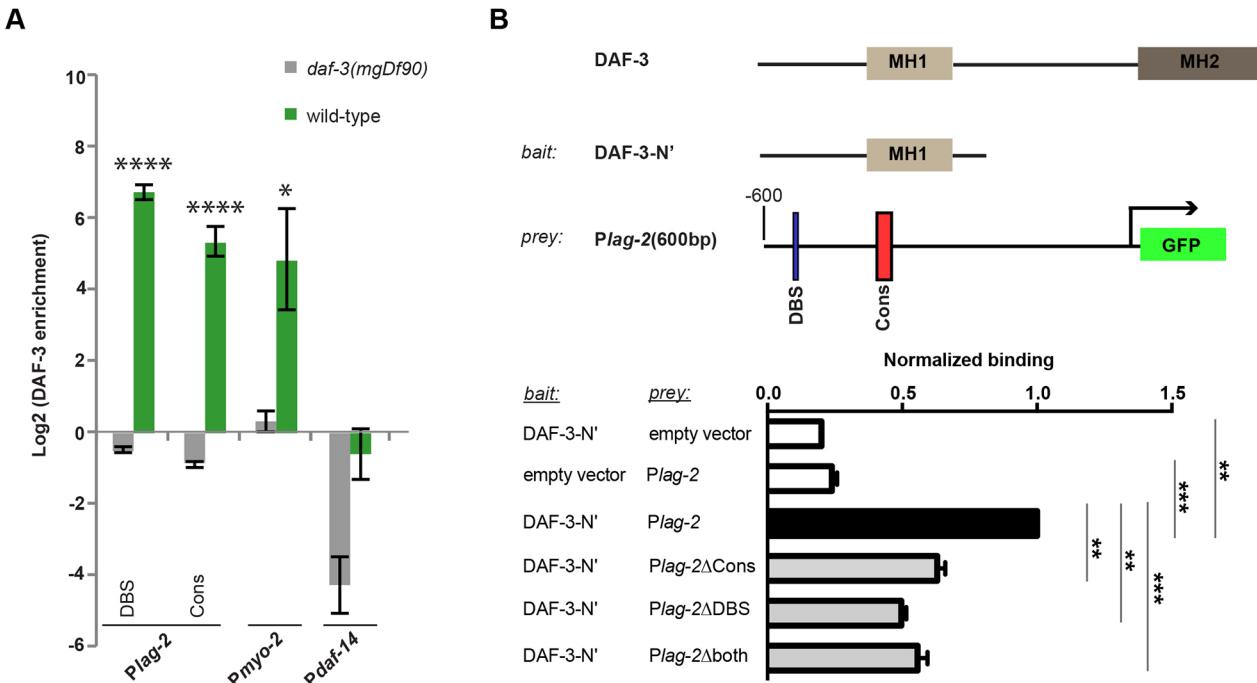


**Fig. 6. DAF-3 can bind the *lag-2* promoter.** (A) Log<sub>2</sub> normalized enrichment of DAF-3 SMAD binding to *lag-2* DBS and conserved (Cons) elements in the wild type and in *daf-3(mgDf90)* mutants. Upstream regulatory regions of *myo-2* and *daf-14* serve as positive and negative controls, respectively. Bar graph represents IP-qPCR data, normalized to DAF-3 enrichment at the actin *act-2* promoter (Park et al., 2010).  $n \geq 2$  biologically independent trials. Significant enrichment in wild type relative to *daf-3(mgDf90)* is indicated by \* $P < 0.05$ , \*\*\* $P < 0.0001$ , two-tailed Student's *t*-test. Data are mean  $\pm$  s.e.m. (B) Bacterial one-hybrid assay. The DAF-3 N-terminal fragment (up to amino acid 250; DAF-3-N') was used as bait and 600 bp upstream of the *lag-2* ATG [Plag-2(600 bp)] was used as prey. Bar graph represents FACS analysis data (mean GFP fluorescence) of different baits and preys, normalized to the signal from DAF-3-N' and Plag-2. Empty prey and bait vectors served as negative controls. Binding of DAF-3-N' to 600 bp of the *lag-2* promoter lacking Cons (Plag-2ΔCons), DBS (Plag-2ΔDBS) or both (Plag-2Δboth). \*\* $P < 0.01$ , \*\*\* $P < 0.001$ , two-tailed Student's *t*-test. Data are mean  $\pm$  s.e.m.

determine how positive regulation by TGF $\beta$  occurs through *cis*-acting sequences upstream of DSL ligand genes *in vivo* in other systems.

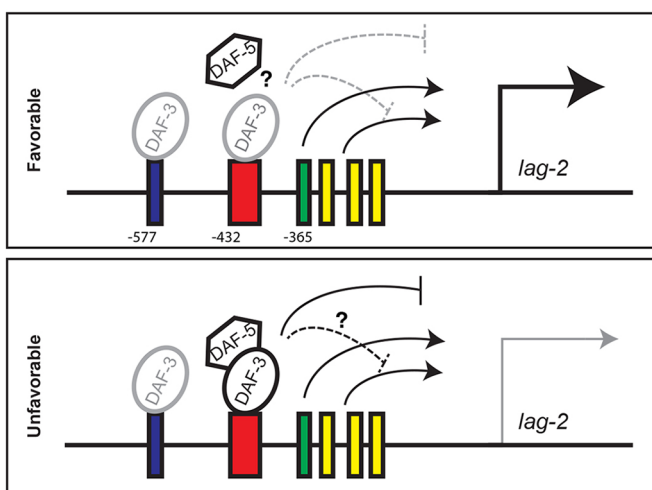


**Fig. 7. A working model for the regulation of late larval DTC-expressed *lag-2*.** (Top) Under favorable conditions, DAF-7/TGF $\beta$  pathway activity inhibits repressor activity of the DAF-3/DAF-5 complex, possibly by interfering with complex formation or stability. *lag-2* expression is driven by positive regulators, including HLH-2, which binds the E-box (green), and unknown regulators that bind other conserved sequences (yellow) shown in Fig. S7. DAF-3 may bind both the DBS (blue) and the Cons (red) sequences under favorable conditions, but it is not active. (Bottom) Under unfavorable conditions, the DAF-3/DAF-5 complex is active and represses *lag-2* expression, possibly by interfering with non-HLH-2 activators. See Discussion for details.

#### Environmental regulation of Notch signaling

Examples of environmental regulation of canonical Notch signaling in response to DSL ligand activity are emerging. In *C. elegans*, LAG-2 is expressed in many different cell types and stages. Expression of *lag-2* in IL2 neurons is dauer specific. This regulation depends on putative forkhead-binding sites 1.3 kb upstream of the start site (Ouellet et al., 2008). In the background of *daf-7* mutants that form dauers constitutively but are still sensitive to dauer recovery cues, Ouellet et al. (2008) found that loss of *lag-2* or *glp-1*, or ablation of IL2, interfered with dauer maintenance. In light of our results, it will be interesting to determine whether the sequences implicated in *lag-2* regulation in the DTC also mediate DAF-3 repression of *lag-2* expression in specific neurons that regulate dauer entry, maintenance and recovery. It is noteworthy that the Cons-binding site we define as crucial for modulation of *lag-2* in the DTC was discovered for its role in the regulation of *osm-9* in postdauer ADL neurons via DAF-3 binding (Sims et al., 2016).

The dauer decision also impacts *lag-2* expression in the context of vulval precursor cell (VPC) fate specification. Here, the DAF-2 pathway, rather than the TGF $\beta$  pathway, transduces environmental signals via inhibition of DAF-16 that acts autonomously to prevent *lag-2* expression in P6.p during dauer and thereby foretells fate specification (Karp and Greenwald, 2013). Regulation of a 1 kb *lag-2* reporter in VPCs (but not in the DTC or in neurons) is also sensitive to *pha-4* RNAi (Chen and Riddle, 2008). Because PHA-4 FOXA acts in both transcriptional regulation and environmental signaling, this regulation may also contribute to the *lag-2* response to environmental cues. It will be interesting to determine whether other (non-LAG-2) DSL ligands in *C. elegans* in other cellular contexts are regulated by the environment.

In *Drosophila*, regulation of Notch signaling by the environment or physiology has been documented in at least two contexts: the ovary and the adult brain. In the ovary, Notch activity is required to maintain somatic cap cells that, in turn, maintain germline stem cells (GSCs) (Song et al., 2007). Under poor nutrient conditions, low insulin signaling allows FOXO to promote expression of the glycosyltransferase Fringe, which, in turn, negatively regulates Notch receptor activity. Insulin signaling in this context also acts in a Notch-independent manner to promote adhesion between the cap cells and the GSCs (Hsu and Drummond-Barbosa, 2009, 2011; Yang et al., 2013). Delta-dependent modulation of Notch activity in the adult *Drosophila* brain occurs in response to several stimuli, including odorants (Lieber et al., 2011), ultimately contributing to changes in the volume of glomeruli and in activity of specific neurons (Kidd and Lieber, 2016; Kidd et al., 2015).

It remains to be determined whether environmental or physiological regulation of Notch signaling is widespread among animals, whether it occurs primarily via modulation of ligand expression and whether direct regulation of ligand expression by TGF $\beta$  is a common mechanism. Environmental regulation of Notch signaling could conceivably contribute to disease states such as developmental defects and cancer, in which aberrant Notch signaling has been implicated (Aster, 2014). Modulation of Notch signaling by the environment or animal physiology may have fewer consequences in relatively fast or highly robust Notch-mediated cell fate decisions. It may be more consequential in circumstances where Notch activity is required over time (e.g. maintenance of developmental states such as dauer, maintenance of stem cells or response to long-term olfactory cues) or in relatively plastic developmental or physiological processes that are important for survival or reproduction and could thereby confer evolutionary advantage.

## MATERIALS AND METHODS

### Strains and plasmids

Strains were derived from N2 wild type (Bristol) and handled using standard methods (Brenner, 1974). Synchronization was performed by 2 h hatch-off as described previously (Pepper et al., 2003). Unless otherwise indicated, worms were grown on OP50 at 20°C. Transgene alleles are noted in figure legends; corresponding plasmids are in Table S1, together with full genotypes of all strains. Plasmids generated for this study were: pGC457, pGC630, pGC642, pGC643, pGC644, pGC680, pGC681, pGC682, pGC683 and pGC684; see Table S1 for plasmid construction details and primer sequences. Transgenic strains were integrated by microparticle bombardment (Praitis et al., 2001) into DP38 *unc-119(ed3)*, except for MosSCI-generated *naSi8* (Frøkjær-Jensen et al., 2008). To compare transgene expression in different mutant backgrounds, each transgene insertion was generated in an otherwise wild-type (non-TGF $\beta$ -pathway mutant) background and subsequently crossed into the different TGF $\beta$  pathway gene mutants.

### Microscopy and image analysis

For fluorescence images, live animals were immobilized with 0.2 mM levamisole in M9 on a 4% agarose pad and imaged at 63 $\times$ /1.20 objective on Leica SP5 confocal microscope. For each experiment, control and experimental animals (e.g. wild type, *daf-7* and *daf-7;daf-3*) were imaged in a single session. All microscope (e.g. laser power, gain, pin hole) and camera settings (e.g. exposure times) were established and held constant for imaging sessions for each transgene. Exposure times and gain were adjusted to insure sub-saturating levels. Approximately 25 images (z-stacks) were captured at intervals of 0.46  $\mu$ m, and were analyzed using ImageJ (<http://rsb.info.nih.gov/ij>). Figures show z-stacks as maximum intensity projections.

### Quantification of *lag-2* reporter expression

After summing the intensity for the entire projection, bandpass filtering and thresholding were performed to help distinguish between DTC and gut

granule signals. The ‘analyze particles’ function was applied and mean pixel intensity was measured in all particles that were manually designated as DTC (i.e. omitting gut granule signals that appear as large bright spots in some figure panels, depending on the orientation of the animal). At least 15 animals were analyzed per genotype.

### Quantification of *lag-2* *in situ* hybridization

The ImageJ ‘object counter 3D’ plug-in was used. The threshold was set such that pixel intensity was measured only from the *in situ* signal, and the pixel intensity from all the detected dots in all stacks in each image was summed. At least 15 animals were analyzed per genotype.

### Germ nuclei counts

Whole-worm fixation, staining, microscopy and proliferative zone determination were performed according to Michaelson et al. (2010). Germ nuclei counts used a semi-automated ImageJ plug-in described previously (Korta et al. 2012).

### *In situ* hybridization

Custom Stellaris fluorescent *in situ* hybridization probes were designed against the cDNA of *lag-2* using the Stellaris FISH Probe Designer (<https://www.biostech.com/support/tools/design-software/stellaris-probe-designer>) and 48 probes labeled with Quasar 670 were obtained from Biosearch Technologies. L4 animals were dissected and subjected to a procedure similar to Biosearch recommendations and to that described by Lee et al. (2016) with modifications as follows: after washing twice with M9 buffer, gonads were fixed (3.7% formaldehyde in 1 $\times$ PBS RNase free) for 45 min at room temperature. Following two washes with 1 $\times$ PBS, gonads were resuspended in 70% ethanol for 30 min. Following ethanol removal, samples were washed in wash buffer (2 $\times$ SSC, 10% deionized formamide) for 5 min. After wash buffer removal, samples were placed in hybridization buffer (228 mM dextran sulfate, 2 $\times$ SSC, 10% deionized formamide) mixed with *lag-2* probe at 0.25  $\mu$ m final concentration at 37°C overnight in the dark. After hybridization solution removal, samples were washed with wash buffer for 30 min at 37°C in the dark. Samples were then washed in 2 $\times$ SSC. Following 2 $\times$ SSC removal, samples were mounted using Antifade Prolong Gold mounting medium (Life Technologies). All solutions were made with nuclease-free water.

### Bacterial reduction and dauer pheromone assays

Both pheromone and food (OP50) assays were performed as described by Dalfó et al. (2012). Synchronized early L3 worms were washed and distributed on plates at 25°C and analyzed in the L4 for *lag-2* DTC expression and as early adults for number of nuclei in the proliferative zone. Pairs of conditions (high/low food and with/without pheromone) were carried out in parallel in at least three independent experiments and, in each case, L4 and adult animals were taken from the same plates to ensure they experienced the same conditions. Bacterial concentrations were established by serial dilutions as described previously (Korta et al., 2012). Dauer pheromone preparation was carried out as described previously (Zhang et al., 2013). In this case, 66  $\mu$ l of crude pheromone was added to 1 ml of NGM agar, the amount that caused 100% of animals to enter dauer in a wild-type population at 25°C.

### Chromatin immunoprecipitation

DAF-3 chromatin immunoprecipitation (ChIP) was performed as described previously (Sims et al., 2016) using Novus Biologicals NB100-1924 Lot A1, and packed worm pellets (~500  $\mu$ l) of N2 L4 larvae. The negative control, which is particularly important for this potentially cross-reactive antibody, was a packed pellet (~500  $\mu$ l) of mixed population GR1311 *daf-3(mgDf90)*.

### Real-time PCR

Quantitative real-time PCR was carried out using 1  $\mu$ l of the DAF-3 ChIP using the iTaq Universal SYBR Green Supermix (BioRad). Primers used were: MO2389 and MO2390 for the region in the *lag-2* promoter homologous to an *osm-9* promoter region with a potential DAF-3 binding site (DBS); MO2391 and MO2388 for the conserved PD motif in the *lag-2* promoter; MO2339 and MO2340 for the DBS in the *osm-9* promoter;

MO2392 and MO2393 for the conserved sequence in the PD motif in the *osm-9* promoter; MO2262 and MO2263 for detection of the C sub-element in the *myo-2* promoter; MO2398 and MO2399 for a region in exon 1 of *lag-2*; and MO2402 and MO2403 for a region in exon 3 of *lag-2* (see Table S1). Regions in the promoters of *daf-7* and *daf-8* were used as positive controls and *daf-14* as a negative control (Park et al., 2010). Ct values were normalized using *act-2* (Park et al., 2010).

### Bacterial one-hybrid assay

Mutant and wild-type versions of the *lag-2* upstream sequence (600 bp) were cloned into MRB1H-reporter vector (also known as 'GHUC', see Table S1) (Oakes et al., 2016) between *NoI* and *EcoRI* upstream of the HIS3-GFP cassette, generating GHUC-1, GHUC-2, GHUC-3, GHUC-4, GHUC-5, GHUC-6 and GHUC-7. DNA encoding amino acids 1-250 of DAF-3 (DAF-3-N') was cloned into the pB1Hw2-omega vector (Noyes et al., 2008) between *KpnI* and *XbaI*, creating an omega-DAF-3-N' fusion in pB1Hw2-Daf3250 (see Table S1). Combinations of the DAF-3-N' pB1Hw2-omega vector or pB1Hw2-Daf3250 (bait) and *lag-2* promoter MRB1H-reporter vectors or GHUC-1 to GHUC-7 (prey) were transformed into USO Aomega cells (Noyes et al., 2008) and selected on Kan/Amp to recover cells with both plasmids. Three replicate colonies from each bait-prey combination were inoculated into 5 ml rich media with Kan/Amp, and incubated at 37°C for ~8 h (OD600=0.5). From each culture, 2.5 µl was used to inoculate 5 ml supplemented minimal NM media containing histidine, uracil, IPTG, Kan/Amp (Noyes et al., 2008) and grown at 37°C overnight (OD600~1.0-2.0). On ice, 1 ml from each sample was pelleted, washed once with PBS and re-pelleted. PBS was removed and the pellet resuspended in 1 ml PBS+1% FBS. Resuspended cells (100 µl) were added to 1.5 ml PBS+1% FBS in a FACS tube. The mean GFP fluorescence of *lag-2* mutant samples and controls and *lag-2* scrambled samples and controls were measured with a Sony SH800 cell sorter and a BD LSRII HTS sorter, respectively. Mean fluorescence values were determined from at least 10,000 cells. Sequences for scrambled *lag-2* DBS and Cons sequences were: 5'-ctatcaact-3' and 5'-ctgcggcaggccactgggct-3', respectively.

### Acknowledgements

We thank Yossi Capua and Jesus Martinez-Gomez for technical assistance, Chris Rushlow for advice, and members of the Nance and Hubbard labs for advice, discussions and comments on the manuscript. Some strains were provided by the CGC, which is funded by NIH Office of Research Infrastructure Programs (P40 OD010440). We also thank WormBase and the NYU School of Medicine's Microscopy Core, which is partially supported by a Cancer Center Support Grant (P30CA016087), for the use of confocal microscope, which is partially supported by NCRR S10 RR024708.

### Competing interests

The authors declare no competing or financial interests.

### Author contributions

Conceptualization: O.P., M.B.N., S.E.H., E.J.A.H.; Methodology: O.P., M.B.N., S.E.H., E.J.A.H.; Validation: O.P., M.C.O., M.B.N., S.E.H., E.J.A.H.; Formal analysis: O.P., M.C.O., M.B.N., S.E.H., E.J.A.H.; Investigation: O.P., M.C.O., K.Y.H.; Resources: O.P., M.C.O., M.B.N., S.E.H., E.J.A.H.; Data curation: O.P., M.B.N., S.E.H., E.J.A.H.; Writing - original draft: O.P., M.B.N., S.E.H., E.J.A.H.; Writing - review & editing: O.P., M.C.O., M.B.N., S.E.H., E.J.A.H.; Visualization: O.P., M.C.O., S.E.H.; Supervision: M.B.N., S.E.H., E.J.A.H.; Project administration: M.B.N., S.E.H., E.J.A.H.; Funding acquisition: E.J.A.H., S.E.H.

### Funding

This work was supported by the National Institutes of Health (R01GM102254 and R01GM061706 to E.J.A.H.; R15GM111094 to S.E.H.). Deposited in PMC for release after 12 months.

### Supplementary information

Supplementary information available online at <http://dev.biologists.org/lookup/doi/10.1242/dev.147660.supplemental>

### References

- Aster, J. C. (2014). In brief: Notch signalling in health and disease. *J. Pathol. 232*, 1-3.
- Austin, J. and Kimble, J. (1987). glp-1 is required in the germ line for regulation of the decision between mitosis and meiosis in *C. elegans*. *Cell* **51**, 589-599.
- Brenner, S. (1974). The genetics of *Caenorhabditis elegans*. *Genetics* **77**, 71-94.
- Chen, N. and Greenwald, I. (2004). The lateral signal for LIN-12/Notch in *C. elegans* vulval development comprises redundant secreted and transmembrane DSL proteins. *Dev. Cell* **6**, 183-192.
- Chen, D. and Riddle, D. L. (2008). Function of the PHA-4/FOXA transcription factor during *C. elegans* post-embryonic development. *BMC Dev. Biol.* **8**, 26.
- Chesney, M. A., Lam, N., Morgan, D. E., Phillips, B. T. and Kimble, J. (2009). *C. elegans* HLH-2/E/Daughterless controls key regulatory cells during gonadogenesis. *Dev. Biol.* **331**, 14-25.
- Dalfó, D., Michaelson, D. and Hubbard, E. J. A. (2012). Sensory regulation of the *C. elegans* germline through TGF-β-dependent signaling in the niche. *Curr. Biol.* **22**, 712-719.
- Deplancque, B., Mukhopadhyay, A., Ao, W., Elewa, A. M., Grove, C. A., Martinez, N. J., Sequerra, R., Doucette-Stamm, L., Reece-Hoyes, J. S., Hope, I. A. et al. (2006). A gene-centered *C. elegans* protein-DNA interaction network. *Cell* **125**, 1193-1205.
- Drummond-Barbosa, D. (2008). Stem cells, their niches and the systemic environment: an aging network. *Genetics* **180**, 1787-1797.
- Frækjær-Jensen, C., Wayne Davis, M., Hopkins, C. E., Newman, B. J., Thummel, J. M., Olesen, S.-P., Grunnet, M. and Jorgensen, E. M. (2008). Single-copy insertion of transgenes in *Caenorhabditis elegans*. *Nat. Genet.* **40**, 1375-1383.
- Greenwald, I. S., Sternberg, P. W. and Horvitz, H. R. (1983). The lin-12 locus specifies cell fates in *Caenorhabditis elegans*. *Cell* **34**, 435-444.
- Gumienny, T. L. (2013). TGF-β signaling in *C. elegans*. In *WormBook* (ed. The *C. elegans* Research Community). WormBook, <http://www.wormbook.org>.
- Henderson, S. T., Gao, D., Lambie, E. J. and Kimble, J. (1994). *lag-2* may encode a signaling ligand for the GLP-1 and LIN-12 receptors of *C. elegans*. *Development* **120**, 2913-2924.
- Hsu, H.-J. and Drummond-Barbosa, D. (2009). Insulin levels control female germline stem cell maintenance via the niche in *Drosophila*. *Proc. Natl Acad. Sci. USA* **106**, 1117-1121.
- Hsu, H.-J. and Drummond-Barbosa, D. (2011). Insulin signals control the competence of the *Drosophila* female germline stem cell niche to respond to Notch ligands. *Dev. Biol.* **350**, 290-300.
- Hubbard, E. J. A., Korta, D. Z. and Dalfó, D. (2012). Physiological control of germline development. In *Germ Cell Development in C. elegans*, pp. 101-131. New York, NY: Springer.
- Hudson, C. and Yasuo, H. (2005). Patterning across the ascidian neural plate by lateral Nodal signalling sources. *Development* **132**, 1199-1210.
- Hudson, C. and Yasuo, H. (2006). A signalling relay involving Nodal and Delta ligands acts during secondary notochord induction in *Ciona* embryos. *Development* **133**, 2855-2864.
- Karp, X. (2003). Post-transcriptional regulation of the E/Daughterless ortholog HLH-2, negative feedback, and birth order bias during the AC/VU decision in *C. elegans*. *Genes Dev.* **17**, 3100-3111.
- Karp, X. and Greenwald, I. (2004). Multiple roles for the E/Daughterless ortholog HLH-2 during *C. elegans* gonadogenesis. *Dev. Biol.* **272**, 460-469.
- Karp, X. and Greenwald, I. (2013). Control of cell-fate plasticity and maintenance of multipotency by DAF-16/FoxO in quiescent *Caenorhabditis elegans*. *Proc. Natl Acad. Sci. USA* **110**, 2181-2186.
- Kidd, S. and Lieber, T. (2016). Mechanism of Notch pathway activation and its role in the regulation of olfactory plasticity in *Drosophila melanogaster*. *PLoS ONE* **11**, e0151279.
- Kidd, S., Struhl, G. and Lieber, T. (2015). Notch is required in adult *Drosophila* sensory neurons for morphological and functional plasticity of the olfactory circuit. *PLoS Genet.* **11**, e1005244.
- Kimble, J. E. and White, J. G. (1981). On the control of germ cell development in *Caenorhabditis elegans*. *Dev. Biol.* **81**, 208-219.
- Korta, D. Z., Tuck, S. and Hubbard, E. J. A. (2012). S6K links cell fate, cell cycle and nutrient response in *C. elegans* germline stem/progenitor cells. *Development* **139**, 859-870.
- Krause, M., Park, M., Zhang, J. M., Yuan, J., Harfe, B., Xu, S. Q., Greenwald, I., Cole, M., Paterson, B. and Fire, A. (1997). A *C. elegans* E/Daughterless bHLH protein marks neuronal but not striated muscle development. *Development* **124**, 2179-2189.
- Kurpinski, K., Lam, H., Chu, J., Wang, A., Kim, A., Tsay, E., Agrawal, S., Schaffer, D. V. and Li, S. (2010). Transforming growth factor-β and notch signaling mediate stem cell differentiation into smooth muscle cells. *Stem Cells* **28**, 734-742.
- Larsen, P. L., Albert, P. S. and Riddle, D. L. (1995). Genes that regulate both development and longevity in *Caenorhabditis elegans*. *Genetics* **139**, 1567-1583.
- Laws, K. M. and Drummond-Barbosa, D. (2017). Control of germline stem cell lineages by diet and physiology. *Results Probl. Cell Differ.* **59**, 67-99.
- Lee, C., Sorensen, E. B., Lynch, T. R. and Kimble, J. (2016). *C. elegans* GLP-1/Notch activates transcription in a probability gradient across the germline stem cell pool. *Elife* **5**, e18370.
- Lieber, T., Kidd, S. and Struhl, G. (2011). DSL-Notch signaling in the *Drosophila* brain in response to olfactory stimulation. *Neuron* **69**, 468-481.

- Michaelson, D., Korta, D. Z., Capua, Y. and Hubbard, E. J. A.** (2010). Insulin signaling promotes germline proliferation in *C. elegans*. *Development* **137**, 671-680.
- Monteiro, R., Pinheiro, P., Joseph, N., Peterkin, T., Koth, J., Repapi, E., Bonkhofer, F., Kirmizitas, A. and Patient, R.** (2016). Transforming growth factor beta drives hemogenic endothelium programming and the transition to hematopoietic stem cells. *Dev. Cell* **38**, 358-370.
- Morikawa, M., Koinuma, D., Tsutsumi, S., Vasilaki, E., Kanki, Y., Hedin, C.-H., Aburatani, H. and Miyazono, K.** (2011). ChIP-seq reveals cell type-specific binding patterns of BMP-specific Smads and a novel binding motif. *Nucleic Acids Res.* **39**, 8712-8727.
- Nadarajan, S., Govindan, J. A., McGovern, M., Hubbard, E. J. A. and Greenstein, D.** (2009). MSP and GLP-1/Notch signaling coordinately regulate actomyosin-dependent cytoplasmic streaming and oocyte growth in *C. elegans*. *Development* **136**, 2223-2234.
- Noyes, M. B.** (2012). Analysis of specific protein-DNA interactions by bacterial one-hybrid assay. *Methods Mol. Biol.* **786**, 79-95.
- Noyes, M. B., Meng, X., Wakabayashi, A., Sinha, S., Brodsky, M. H. and Wolfe, S. A.** (2008). A systematic characterization of factors that regulate Drosophila segmentation via a bacterial one-hybrid system. *Nucleic Acids Res.* **36**, 2547-2560.
- Oakes, B. L., Xia, D. F., Rowland, E. F., Xu, D. J., Ankoudinova, I., Borchardt, J. S., Zhang, L., Li, P., Miller, J. C., Rebar, E. J. et al.** (2016). Multi-reporter selection for the design of active and more specific zinc-finger nucleases for genome editing. *Nat. Commun.* **7**, 10194.
- Ouellet, J., Li, S. and Roy, R.** (2008). Notch signalling is required for both dauer maintenance and recovery in *C. elegans*. *Development* **135**, 2583-2592.
- Park, D., Estevez, A. and Riddle, D. L.** (2010). Antagonistic Smad transcription factors control the dauer/non-dauer switch in *C. elegans*. *Development* **137**, 477-485.
- Patterson, G. I., Koweeek, A., Wong, A., Liu, Y. and Ruvkun, G.** (1997). The DAF-3 Smad protein antagonizes TGF-beta-related receptor signaling in the *Caenorhabditis elegans* dauer pathway. *Genes Dev.* **11**, 2679-2690.
- Pepper, A. S.-R., Kilian, D. J. and Hubbard, E. J. A.** (2003). Genetic analysis of *Caenorhabditis elegans* glp-1 mutants suggests receptor interaction or competition. *Genetics* **163**, 115-132.
- Praitis, V., Casey, E., Collar, D. and Austin, J.** (2001). Creation of low-copy integrated transgenic lines in *Caenorhabditis elegans*. *Genetics* **157**, 1217-1226.
- Ren, P., Lim, C. S., Johnsen, R., Albert, P. S., Pilgrim, D. and Riddle, D. L.** (1996). Control of *C. elegans* larval development by neuronal expression of a TGF-beta homolog. *Science* **274**, 1389-1391.
- Richards, G. S. and Degnan, B. M.** (2010). The dawn of developmental signaling in the Metazoa. *Cold Spring Harb. Symp. Quant. Biol.* **74**, 81-90.
- Schackwitz, W. S., Inoue, T. and Thomas, J. H.** (1996). Chemosensory neurons function in parallel to mediate a pheromone response in *C. elegans*. *Neuron* **17**, 719-728.
- Seydoux, G., Schedl, T. and Greenwald, I.** (1990). Cell-cell interactions prevent a potential inductive interaction between soma and germline in *C. elegans*. *Cell* **61**, 939-951.
- Shin-i, T. and Kohara, Y.** (1999). NEXTDB: the expression pattern map database for *C. elegans*. *Genome Inform.* **10**, 213-214.
- Sijen, T., Fleenor, J., Simmer, F., Thijssen, K. L., Parrish, S., Timmons, L., Plasterk, R. H. and Fire, A.** (2001). On the role of RNA amplification in dsRNA-triggered gene silencing. *Cell* **107**, 465-476.
- Sims, J. R., Ow, M. C., Nishiguchi, M. A., Kim, K., Sengupta, P. and Hall, S. E.** (2016). Developmental programming modulates olfactory behavior in *C. elegans* via endogenous RNAi pathways. *Elife* **5**, e11642.
- Singh, K., Chao, M. Y., Somers, G. A., Komatsu, H., Corkins, M. E., Larkins-Ford, J., Tucey, T., Dionne, H. M., Walsh, M. B., Beaumont, E. K. et al.** (2011). *C. elegans* notch signaling regulates adult chemosensory response and larval molting quiescence. *Curr. Biol.* **21**, 825-834.
- Song, X., Call, G. B., Kirilly, D. and Xie, T.** (2007). Notch signaling controls germline stem cell niche formation in the *Drosophila* ovary. *Development* **134**, 1071-1080.
- Starich, T. A., Hall, D. H. and Greenstein, D.** (2014). Two classes of gap junction channels mediate soma-germline interactions essential for germline proliferation and gametogenesis in *Caenorhabditis elegans*. *Genetics* **198**, 1127-1153.
- Thatcher, J. D., Haun, C. and Okkema, P. G.** (1999). The DAF-3 Smad binds DNA and represses gene expression in the *Caenorhabditis elegans* pharynx. *Development* **126**, 97-107.
- Yang, S.-A., Wang, W.-D., Chen, C.-T., Tseng, C.-Y., Chen, Y.-N. and Hsu, H.-J.** (2013). FOXO/Fringe is necessary for maintenance of the germline stem cell niche in response to insulin insufficiency. *Dev. Biol.* **382**, 124-135.
- Zavadil, J., Cermak, L., Soto-Nieves, N. and Böttiger, E. P.** (2004). Integration of TGF-beta/Smad and Jagged1/Notch signalling in epithelial-to-mesenchymal transition. *EMBO J.* **23**, 1155-1165.
- Zhang, X., Noguez, J. H., Zhou, Y. and Butcher, R. A.** (2013). Analysis of ascarosides from *Caenorhabditis elegans* using mass spectrometry and NMR spectroscopy. *Methods Mol. Biol.* **1068**, 71-92.

## SUPPLEMENTARY INFORMATION

### SUPPLEMENTARY MATERIALS AND METHODS

#### **RNAi experiments and germ cell counts:**

RNAi by bacterial feeding was performed as described (Timmons et al., 2001).

*lin-12* RNAi [Ahringer clone sjj\_R107.8; (Kamath et al., 2003)] in N2, *rrf-1(pk1417)* and *rrf-3(pk1426)* strains: Animals were fed control (L4440) or *lin-12* RNAi for two generations: after L1 synchronization by hatch-off, early adults (prior to egg-laying) were transferred to new RNAi plates overnight and then removed to limit progeny that were then scored as early adults. RNAi experiments evaluated for vulval morphology were scored in one generation as adults after L1 hatch-off onto RNAi plates.

*hlh-2* RNAi: Two *hlh-2* RNAi clones were created according to (Chesney et al., 2009).

Synchronized early third larval stage worms (L3) were fed control (L4440) or *hlh-2* RNAi clones and scored as fourth larval stage worms (L4) for *lag-2* DTC expression analysis or as early adults to count the number of nuclei in the proliferative zone. Similarly to (Chesney et al., 2009), two *hlh-2* RNAi clones showed similar effects and were analyzed together.

**Germ nuclei counts:** See main text for methods used to determine germ nuclei counts in the proliferative zone.

**TABLE S1****A. Strains used in this study:**

<b>Strain</b>	<b>Genotype</b>	<b>Reference</b>
N2	Wild-type	(Brenner, 1974)
CB1372	<i>daf-7(e1372)</i>	(Swanson and Riddle, 1981)
DR40	<i>daf-1(m40)</i>	(Swanson and Riddle, 1981)
GR1269	<i>daf-7(e1372); daf-3(e1376)</i>	(da Graca et al., 2004)
GC1147	<i>daf-1(m40); daf-3(e1376)</i>	(Dalfo et al., 2012)
GC1149	<i>daf-5(e1386); daf-1(m40)</i>	(Dalfo et al., 2012)
GC832	<i>glp-1(e2141)</i>	(Hutter and Schnabel, 1994)
PD8488	<i>rrf-1(pk1417)</i>	(Sijen et al., 2001)
NL2099	<i>rrf-3(pk1426)</i>	(Simmer et al., 2003)
NF2168	<i>tkIs11 [Pmig-24::Venus ]</i>	(Tamaï and Nishiwaki, 2007)
GR1311	<i>daf-3(mgDf90)</i>	(Patterson et al., 1997)
GC909	<i>rrf-1(pk1417); glp-1(e2141)</i>	(Korta et al., 2012)
GC1172	<i>xnSi1[Pmex-5::GFP-PH:: nos-2(3')] II; unc-119(ed3); nals37[pGC457 Plag-2(3kb)::mCherry-PH::let-858(3'); unc-119(+)]</i>	(Chihara and Nance, 2012); This study
GC1412	<i>naSi8 [pGC680 Plag-2(3kb)::GFP-PH::let-858(3')] II</i>	This study
GC1418	<i>daf-7(e1372); naSi8 [pGC680 Plag-2(3kb)::GFP-PH::let-858(3')] II</i>	This study
GC1419	<i>daf-7(e1372); daf-3(e1376); naSi8 [pGC680 Plag-2(3kb)::GFP-PH::let-858(3')] II</i>	This study
GC1420	<i>daf-1(m40); xnSi1[Pmex-5::GFP-PH:: nos-2(3')] II; unc-119(ed3); nals37[pGC457 Plag-2(3kb)::mCherry-PH::let-858(3'); unc-119(+)]</i>	This study
GC1421	<i>daf-5(e1386); daf-1(m40); xnSi1[Pmex-5::GFP-PH:: nos-2(3')] II; unc-119(ed3); nals37[pGC457 Plag-2(3kb)::mCherry-PH::let-858(3'); unc-119(+)]</i>	This study
GC1347	<i>unc-119(ed3); nals81[pGC630 Plag-2(2kb)::GFP-PH::let-858(3'); unc-119(+)]</i>	This study
GC1349	<i>daf-7(e1372); unc-119(ed3); nals81[pGC630 Plag-2(2kb)::GFP-PH::let-858(3'); unc-119(+)]</i>	This study
GC1359	<i>unc-119(ed3); nals84[pGC642 Plag-2(1kb)::GFP-PH::let-858(3'); unc-119(+)]</i>	This study
GC1362	<i>unc-119(ed3); nals87[pGC643 Plag-2(0.5kb)::GFP-PH::let-858(3'); unc-119(+)]</i>	This study
GC1422	<i>daf-7(e1372); daf-3(e1376); unc-119(ed3); nals81[pGC630 Plag-2(2kb)::GFP-PH::let-858(3'); unc-119(+)]</i>	This study

GC1423	<i>daf-7(e1372); unc-119(ed3); nals84[pGC642 Plag-2(1kb)::GFP-PH::let-858(3'); unc-119(+)]</i>	This study
GC1424	<i>daf-7(e1372); daf-3(e1376); unc-119(ed3); nals84[pGC642 Plag-2(1kb)::GFP-PH::let-858(3'); unc-119(+)]</i>	This study
GC1425	<i>daf-7(e1372); unc-119(ed3); nals87[pGC643 Plag-2(0.5kb)::GFP-PH::let-858(3'); unc-119(+)]</i>	This study
GC1426	<i>daf-7(e1372); daf-3(e1376); unc-119(ed3); nals87[pGC643 Plag-2(0.5kb)::GFP-PH::let-858(3'); unc-119(+)]</i>	This study
GC1427	<i>unc-119(ed3); nals96[pGC644 mutPlag-2(3kb)::GFP-PH::let-858(3'); unc-119(+)]</i>	This study
GC1429	<i>naSi8 [pGC680 Plag-2(3kb)::GFP-PH::let-858(3')] II; unc-119(ed3); nals96[pGC644 mutPlag-2(3kb)::GFP-PH::let-858(3'); unc-119(+)]</i>	This study
GC1430	<i>daf-7(e1372); naSi8 [pGC680 Plag-2(3kb)::GFP-PH::let-858(3')] II; unc-119(ed3); nals96[pGC644 mutPlag-2(3kb)::GFP-PH::let-858(3'); unc-119(+)]</i>	This study
GC1431	<i>unc-119(ed3) ;nals98[pGC681 Plag-2(405bp)::GFP-PH::let-858(3'); unc-119(+)]</i>	This study
GC1433	<i>daf-7(e1372); unc-119(ed3); nals98[pGC681 Plag-2(405bp)::GFP-PH::let-858(3'); unc-119(+)]</i>	This study
GC1434	<i>daf-7(e1372); daf-3(e1376); unc-119(ed3); nals98[pGC681 Plag-2(405bp)::GFP-PH::let-858(3'); unc-119(+)]</i>	This study
GC1435	<i>unc-119(ed3); nals100[pGC682 Plag-2(1kbΔDBS)::GFP-PH::let-858(3'); unc-119(+)]</i>	This study
GC1437	<i>daf-7(e1372); unc-119(ed3); nals100[pGC682 Plag-2(1kbΔDBS)::GFP-PH::let-858(3'); unc-119(+)]</i>	This study
GC1438	<i>daf-7(e1372); daf-3(e1376); unc-119(ed3); nals100[pGC682 Plag-2(1kbΔDBS)::GFP-PH::let-858(3'); unc-119(+)]</i>	This study
GC1439	<i>unc-119(ed3); nals102[pGC683 Plag-2(1kbΔCons)::GFP-PH::let-858(3'); unc-119(+)]</i>	This study
GC1443	<i>daf-7(e1372); unc-119(ed3); nals102[pGC683 Plag-2(1kbΔCons)::GFP-PH::let-858(3'); unc-119(+)]</i>	This study
GC1445	<i>daf-7(e1372); daf-3(e1376); unc-119(ed3);nals102[pGC683 Plag-2(1kbΔCons)::GFP-PH::let-858(3'); unc-119(+)]</i>	This study
GC1447	<i>unc-119(ed3); nals106[pGC684 Plag-2(1kbΔDBS+ΔCons)::GFP-PH::let-858(3'); unc-119(+)]</i>	This study

GC1450	<i>daf-7(e1372); unc-119(ed3); nals106[pGC684 Plag-2(1kbΔDBS+ΔCons)::GFP-PH::let-858(3'); unc-119(+)]</i>	This study
GC1451	<i>daf-7(e1372); daf-3(e1376); unc-119(ed3); nals106[pGC684 Plag-2(1kbΔDBS+ΔCons)::GFP-PH::let-858(3'); unc-119(+)]</i>	This study
GC1452	<i>daf-7(e1372); xnSi1[Pmex-5::GFP-PH:: nos-2(3')] II; unc-119(ed3); nals37[pGC457 Plag-2(3kb)::mCherry-PH::let-858(3'); unc-119(+)]</i>	This study
GC1453	<i>daf-1(m40); daf-3(e1376); xnSi1[Pmex-5::GFP-PH:: nos-2(3')] II; unc-119(ed3); nals37[pGC457 Plag-2(3kb)::mCherry-PH::let-858(3'); unc-119(+)]</i>	This study

## B. Plasmids used in this study:

Plasmid	Description	Reference/Construction
pPD129.36	Control RNAi (L4440)	(Timmons and Fire, 1998)
sjj_R107.8	<i>lin-12(RNAi)</i>	(Kamath et al., 2003)
pGC457	<i>Plag-2(3kb)::mCherry-PH::let-858(3')</i>	GFP-let-858 was cut out from pPD117.01 using AgeI/Apal and inserted into pJK590. The resulting plasmid was then cut with SmaI/SpeI and ligated with mCherry-PH, which was cut with SpeI from pDC05 (Chihara and Nance, 2012).
pGC630	<i>Plag-2(2kb)::GFP-PH::let-858(3')</i>	A 2kb fragment of the <i>lag-2</i> promoter was amplified from pGC457 using primers GCo1928 and GCo1907. A fragment containing GFP-PH was amplified using primers GCo1909 and GCo1910. The 3' UTR of <i>let-858</i> was amplified from pGC399 (McGovern et al., 2009) using GCo1911 and GCo1912. All the pieces were ligated into pJN566

		(Armenti et al., 2014), digested with Pmel, using Gibson assembly.
pGC642	<i>Plag-2(1kb)::GFP-PH::let-858(3')</i>	A 1kb fragment of the <i>lag-2</i> promoter was amplified from pGC457 using primers GCo1930 and GCo1907. GFP-PH was amplified from pGC630 using GCo1909 and GCo1910. The 3' UTR of <i>let-858</i> was amplified from pGC457 using GCo1911 and GCo1912. All the pieces were ligated into pJN566, digested with Pmel, using Gibson assembly.
pGC643	<i>Plag-2(0.5kb)::GFP-PH::let-858(3')</i>	A 0.5kb fragment of the <i>lag-2</i> promoter was amplified from pGC457 using primers GCo1931 and GCo1907. GFP-PH was amplified from pGC630 using GCo1909 and GCo1910. 3' UTR of <i>let-858</i> was amplified from pGC457 using GCo1911 and GCo1912. All the pieces were ligated into pJN566, digested with Pmel, using Gibson assembly.
pGC644	<i>mutPlag-2(3kb)::mCherry-PH::let-858(3')</i>	pGC457 was mutagenized using site-directed mutagenesis with Pfu polymerase. 3 pairs of primers were used: GCo1866 and GCo1867, GCo1868 and GCo1869, GCo1870 and GCo1871.
pGC680	<i>Plag-2(3kb)::GFP-PH::let-858(3')</i>	A 3kb fragment of the <i>lag-2</i> promoter was amplified from pGC457 using primers GCo1906 and

		GCo1907. GFP-PH was amplified from pGC630 using GCo1909 and GCo1910. 3' UTR of <i>let-858</i> was amplified from pGC457 using GCo1911 and GCo1912 primers. All the pieces were ligated into pJN566, digested with PmeI, using Gibson assembly.
pGC681	<i>Plag-2(450bp)::GFP-PH::let-858(3')</i>	The vector was amplified from pGC642 using primers GCo2149 and GCo2147 and self-ligated using T4-DNA ligase.
pGC682	<i>Plag-2(1kbΔDBS)::GFP-PH::let-858(3')</i>	The vector was amplified from pGC642 using primers GCo2145 and GCo2146 and was ligated with gBlock GCo2383 using Gibson assembly.
pGC683	<i>Plag-2(1kbΔCons)::GFP-PH::let-858(3')</i>	The vector was amplified from pGC642 using primers GCo2145 and GCo2146 and was ligated with gBlock GCo2384 using Gibson assembly.
pGC684	<i>Plag-2(1kbΔDBS+ΔCons)::GFP-PH::let-858(3')</i>	The vector was amplified from pGC642 using primers GCo2145 and GCo2146 and was ligated with gBlock GCo2385 using Gibson assembly.
GHUC-1	<i>Plag-2(600bp) prey</i>	600 bp upstream of the <i>lag-2</i> ATG was purchased as a gBlock ( <i>Lag2 wt</i> ), digested and cloned between the NotI and EcoRI restriction sites of the GHUC reporter vector (see below), placing the fragments upstream of the HIS3-GFP cassette. See additional notes regarding

		B1H vectors in D below.
GHUC-2	<i>Plag-2ΔDBS</i> prey	600 bp upstream of the <i>lag-2</i> ATG was amplified from pGC682 using primers <i>Lag2 600 5p</i> and <i>Lag2 600 3p</i> listed below. These were digested and cloned between the NotI and EcoRI restriction sites of the GHUC reporter vector. See additional notes regarding B1H vectors in D below.
GHUC-3	<i>Plag-2ΔCons</i> prey	600 bp upstream of the <i>lag-2</i> ATG was amplified from pGC683 using primers <i>Lag2 600 5p</i> and <i>Lag2 600 3p</i> listed below. These were digested and cloned between the NotI and EcoRI restriction sites of the GHUC reporter vector. See additional notes regarding B1H vectors in D below.
GHUC-4	<i>Plag-2Δboth</i> prey	600 bp upstream of the <i>lag-2</i> ATG was amplified from pGC684 using primers <i>Lag2 600 5p</i> and <i>Lag2 600 3p</i> listed below. These were digested and cloned between the NotI and EcoRI restriction sites of the GHUC reporter vector.
GHUC-5	<i>Plag-2scrDBS</i> prey	600 bp upstream of the <i>lag-2</i> ATG was purchased as a gBlock with the DBS sequence scrambled ( <i>Lag-2-scrDBS</i> ), digested and cloned between the NotI and EcoRI restriction sites of the GHUC reporter vector. See additional notes regarding B1H

		vectors in D below.
GHUC-6	<i>Plag-2-scrCons</i> prey	600 bp upstream of the <i>lag-2</i> ATG was purchased as a gBlock with the Cons sequence scrambled ( <i>Lag-2-scrCons</i> ), digested and cloned between the <i>NotI</i> and <i>EcoRI</i> restriction sites of the GHUC reporter vector. See additional notes regarding B1H vectors in D below.
GHUC-7	<i>Plag-2-scrBoth</i> prey	600 bp upstream of the <i>lag-2</i> ATG was purchased as a gBlock with the DBS and Cons sequences scrambled ( <i>Lag-2-scrBoth</i> ), digested and cloned between the <i>NotI</i> and <i>EcoRI</i> restriction sites of the GHUC reporter vector. See additional notes regarding B1H vectors in D below.
pB1Hw2-Daf3250	DAF-3-N' bait	The coding sequence of amino acids 1-250 of Daf3 were amplified with primers <i>Daf3 5p</i> and <i>Daf3 250 3p</i> from clone # F25E2.5C of the transcription factors collection from Open Biosystems, catalog # OCE4818-202528301. The coding sequence for these amino acids and an N-terminal linker were cloned between the <i>NotI</i> and <i>XbaI</i> sites of the pB1Hw2 vector. See additional notes regarding B1H vectors in D below.
pGC692	<i>hlh-2</i> RNAi 5' clone	A 5' fragment of the <i>hlh-2</i> mRNA was amplified using primers GCo2416 and

		GC02417 (according to (Chesney et al., 2009). pPD129.26 was digested with EcoRV and ligated with <i>hh-2</i> fragment using Gibson assembly.
pGC693	<i>hh-2</i> RNAi 3' clone	A 3' piece of the <i>hh-2</i> mRNA was amplified using primers GCo2418 and GCo2419 (according to (Chesney et al., 2009). pPD129.26 was digested with EcoRV and ligated with <i>hh-2</i> fragment using Gibson assembly.

### C. Primers and gBlocks used in this study:

Name	Sequence
GCo1866	cgctcaaataaatgtccag
GCo1867	GGAATGCATTGAACATGAGAAG
GCo1868	GTTTGTTCCTTCCCCTTCCC
GCo1869	ggaaaatggctgatggccttg
GCo1870	ggtgtgagtgaagatccttgg
GCo1871	gccggaaaactaaaaatg
GCo1906	aagattttcattagagaatgtctagaactagGCCGTTactggcgctactccacc ttt
GCo1907	cggcaaaattgaaaagtgttgtggctctagcaaagctcaaggcgactataagtt cg
GCo1909	tttcctctaagtatcccgaaacttatagtcgaccttgagcttgcataagccaaca
GCo1910	ttaaaattgaaaattcaacgacgtggcgctgatcatcctaTTTGTATAGTTCA TCCA
GCo1911	TGCTGGGATTACACATGGCATGGATGAACATACAAAtaaggatgt cgacgccaacgtc
GCo1912	CGCACCGTAGCTCGAGTgtaaaacgacggccagtGTTccaagcgagg acaattctca
GCo1928	aagattttcattagagaatgtctagaactagGCCGTTttcggAACgtctcatta ca
GCo1930	aagattttcattagagaatgtctagaactagGCCGTTtaaattagttcgaatt cc
GCo1931	aagattttcattagagaatgtctagaactagGCCGTTgcctgcctatctataacc ta
GCo2145	cgacgaacgacttgtcaataaaaattg
GCo2146	ccttgtcagtcgtcaagaacatac
GCo2147	AAACGGCctagttagacattctc
GCo2149	5' Phos-ctctcaagtattttcacacgtac

GCo2383	cagataaattgcacaattttattgcacaagtcgtcgccgtgtttttaaaatgttggcaaagattgtgaagtccctgttagttaacactctaagttactccaaagactctacctgcctacgcctatcataaccctagtcgttatcacctactcgctgcatagttgatgtacctatataacagttcataaatgaatttgtcaaaaattccactctcaagtatttttacacgtacttatttgacaaatcctgtcagtcgtcaagaacacatcacatcgaaaggcgcaat
GCo2384	cagataaattgcacaattttattgcacaagtcgtcgccgtgttttgcgtcaaatgtggcaaagattgtgaagtccctgttagttaacactctaagttactccaaagactctacctgcctacgcctatcataaccctagtcgttatcacctactcgctgcatagttgatgtacctatataacagtcactctcaagtatttttacacgtacttatttgacaaatcctgtcagtcgtcaagaacacatcacatcgaaaggcgcaat
GCo2385	cagataaattgcacaattttattgcacaagtcgtcgccgtgtttttaaaatgttggcaaagattgtgaagtccctgttagttaacactctaagttactccaaagactctacctgcctacgcctatcataaccctagtcgttatcacctactcgctgcatagttgatgtacctatataacagtcactctcaagtatttttacacgtacttatttgacaaatcctgtcagtcgtcaagaacacatcacatcgaaaggcgcaat
GCo2416	aattaatacgactcactatagggagaccggcagatctgatggcgatccaaatagccaacttacg
GCo2417	cggccccccctcgaggtcgacggtatcgataagctgatcttctgaaggtggaggtaacc
GCo2418	aattaatacgactcactatagggagaccggcagatctgatggcttggagataccaacttg
GCo2419	cggccccccctcgaggtcgacggtatcgataagctgataaaccgtggatgtccaaactgcgc
Daf3 5p	aataaaGCGCCGCGGACTACAAGGATGACGACGACAAGTTCCGGACCGTTCCAAGACACCCCCCATGGTACCAAGCTAATAGCAACTTCTCTTC
Daf3 250 3p	ggcggtTCTAGACTTACCTCTGCCAACAAATCATAGT
Lag2 600 5p	aataaaGCGCCGCAAATAATTGCACAATTTTATTGC
Lag2 600 3p	ccgcccGAATTCTTCTGAAAAAAGGCAAATTG
gBlock: <i>Lag2 wt</i>	aataaaGCGCCGCAAATAATTGCACAATTTTATTGCACAAGTCGTTCGTCGTTCTGTTTTTCGCTGTCAAATGTTGGCAAAGATTGTGAAGTCCCCTGTAGTTAACACTCTAAGTTACTCCAAAGACTTCTACCTGCCTACCTGCCTGCCTATCTATAACCTAGTGCCTATCACC TACTCGCTGCATAGTTGATGTACCTATAAACAGTTCAAAATGAATTTGTCAAATCCACTCTCAAGTATTCTACACGTACTTATTGTACAAATCTTGTACAATCCTTGTCAGTCGCTGCAAGAACATACACATCGAAGAGGCGCAATCGAAACACAGGTGTTGCCGTTGATCGTCTCCCGCCCCGCCTGTTGGCGGGACGGGTGTCGGTCACCACCACATCATATTGTTGGACACACTTGCACATCCGGTTCACACCCGATTACCGCATCGGGGCTTGATCTGGGGCGGTATTGGATCTTTGTTATGTAGATTTTCTCGCCGTTATGATTGGATTATTTTCTCTTATCTTGAGACTTGTAATCTTGCCTGATTGCTAGCTAGCCA AAACTTCACTGTTCTTTTCTCTCTAAGTATTCCCAGACTTATAGTCGACCTTGAGCTTGCTAGAAGCCAACAACACTTTCAAAATTGCCCTTTTCAAGAAAGAATTCCcgccc
gBlock: <i>Lag-2-scrDBS</i>	aataaaGCGCCGCAAATAATTGCACAATTTTATTGCACAAGTCGTTCGTCGTTCTGTTTTTCGCTGTCAAATGTTGGCAAAGATTGTGAAGTCCCCTGTAGTTAACACTCTAAGTTACTCCAAAGACTTCTACCTGCCTACCTGCCTGCCTATCTATAACCTAGTGCCTATCACCTACTCGCTGCATAGTTGATGTACCTATAACAGTTCAAAATGAAT

	TTTGTCAAAATTCCACTCTCAAGTATTCTACACGTACTTATTTGT ACAAATCCTGTCAGTCGCTGCAAGAACATACACATCGAAGAGGC GCAATCGAAACAACAGGTGTCGCCCGTTGATCGTCTCCCCGCC CCGCCTGTTGGCGGGACGGGTGTCGGTCACCACCAACATCA TATTGTTGGACACACTTGACATCCGGTTACACCCGATTACCG CATCGGGGTCTTGATCTGGGGCGGCTATTGGATCTTTGTTATG TAGATTTTTCTCGCCGTTATGATTTGGATTATTTCTCTTAT CTTGCAGTCGACTTGTAAATCTTGCCTGATTGCTAGCTAGCCAAA ACTTCACTTGTCTTTCTCTAAGTATTTCCCAGACTTAT AGTCGACCTTGAGCTTGCTAGAAGCCAACAACACTTTCAAATT GCCTTTTCAGAAAGAATTCCcgccc
gBlock <i>Lag-2</i> -scrCons	aataaaGCGGCCGCAAATAAATTGACAATTATTGACAAGTC GTTCGTCGTTCTGTTTTTCGCTGTCAAATGTTGGCAAAGATT GTGAAGTCCCCTGTAGTTAACACTCTAAGTTACTCCAAAGACTT CTACCTGCCTACCTGCCTGCCTATCTATAACCTAGTGCCTATCACC TACTCGCTGCATAGTTGATGTACCTATATAACAGT <b>ctgcgggca</b> <b>gccccactggggcct</b> CACTCTCAAGTATTCTACACGTACTTATTTG TACAAATCCTGTCAGTCGCTGCAAGAACATACACATCGAAGAGG CGCAATCGAAACAACAGGTGTCGCCCGTTGATCGTCTCCCCGC CCGCCTGTTGGCGGGACGGGTGTCGGTCACCACCAACATC ATATTGTTGGACACACTTGACATCCGGTTACACCCGATTACC GCATCGGGGTCTTGATCTGGGGCGGCTATTGGATCTTTGTTAT GTAGATTTTTCTCGCCGTTATGATTTGGATTATTTCTCTTA TCTTGCAGTCGACTTGTAAATCTTGCCTGATTGCTAGCTAGCCAA AACTTCACTTGTCTTTCTCTAAGTATTTCCCAGACTTAA TAGTCGACCTTGAGCTTGCTAGAAGCCAACAACACTTTCAAATT TGCCTTTTCAGAAAGAATTCCcgccc
gBlock: <i>Lag-2</i> -scrBoth	aataaaGCGGCCGCAAATAAATTGACAATTATTGACAAGTC GTTCGTCGTTCTGTTTT <b>ctatact</b> AAAATGTTGGCAAAGATTG TGAAGTCCCCTGTAGTTAACACTCTAAGTTACTCCAAAGACTTCT ACCTGCCTACCTGCCTGCCTATCTATAACCTAGTGCCTATCACCTA CTCGCTGCATAGTTGATGTACCTATATAACAGT <b>ctgcgggcaaggc</b> <b>cccaactggggcct</b> CACTCTCAAGTATTCTACACGTACTTATTTGTA CAAATCCTGTCAGTCGCTGCAAGAACATACACATCGAAGAGGCG CAATCGAAACAACAGGTGTCGCCCGTTGATCGTCTCCCCGCC GCCTGTTGGCGGGACGGGTGTCGGTCACCACCAACATCATA TTGTTGGACACACTTGACATCCGGTTACACCCGATTACCGCA TCGGGGTCTGATCTGGGGCGGCTATTGGATCTTTGTTATGTA GATTTTTCTCGCCGTTATGATTTGGATTATTTCTCTTATCT TGCAGTCGACTTGTAAATCTTGCCTGATTGCTAGCTAGCCAAAC TTTCACTTGTCTTTCTCTAAGTATTTCCCAGACTTATAG TCGACCTTGAGCTTGCTAGAAGCCAACAACACTTTCAAATTG CCTTTTCAGAAAGAATTCCcgccc
M02389	gcacaagtgcgtcggtcg
M02390	gggacttcacaatcttgccaac
M02391	acgtgtagaatacttgagagt
M02388	atgtacctatataacagttcataaatg
M02339	tgcgtgttatattatc
M02340	taaagagtggtgaaa
M02392	tttccaccaactcttaatttc

MO2393	aacttccaccgccccatgttg
MO2262	cacactgtactcattgttctg
MO2263	aggttaactaaagatagtgaag
MO2398	ctgtgacatcggtatggatggac
MO2399	ccgtcggttcgcattgagcac
MO2402	gatgaggaagtggatattaccag
MO2403	acgcatactcattattcgattc

#### D. Additional Notes on B1H plasmids:

MRB1H vector (Kanamycin) based plasmids: There are multiple reporters in this vector including GFP, HIS3, URA3, and mCherry (G-H-U-C). For this study we utilized the HIS3-GFP cassette and were only concerned with the activation of GFP. We cloned our inserts between NotI and EcoRI placing them upstream of the promoter that drives the HIS3-GFP cassette. When activated by recruitment of polymerase, HIS3 and GFP are transcribed from the same promoter but an internal Shine-Dalgarno sequence allows each protein to be translated separately.

pB1Hw2 vector (Ampicillin) based plasmids: As first described in (Noyes et al., 2008), the pB1Hw2 vector allows for the expression of a protein of interest as a C-terminal fusion to the omega subunit of bacterial polymerase. In this way omega functions as the activation domain by recruiting the rest of the polymerase only when the protein of interest binds a DNA sequence near a promoter. The “w2” version of this plasmid signifies the use of a weak promoter to drive expression of the omega – protein of interest fusion (w5 and wL versions of the plasmid exist for higher levels of expression). The protein of interest and a stop codon are typically cloned between the KpnI and XbaI sites of the plasmid for in-frame expression. However, in the case of Daf3, there is an internal KpnI site so we cloned into the upstream NotI sequence, recreating the linker between NotI and KpnI on the primer utilized.

## SUPPLEMENTARY REFERENCES

- Armenti, S. T., Lohmer, L. L., Sherwood, D. R. and Nance, J.** (2014). Repurposing an endogenous degradation system for rapid and targeted depletion of *C. elegans* proteins. *Development* **141**, 4640-4647.
- Brenner, S.** (1974). The genetics of *Caenorhabditis elegans*. *Genetics* **77**, 71-94.
- Chesney, M. A., Lam, N., Morgan, D. E., Phillips, B. T. and Kimble, J.** (2009). *C. elegans* HLH-2/E/Daughterless controls key regulatory cells during gonadogenesis. *Developmental Biology* **331**, 14-25.
- Chihara, D. and Nance, J.** (2012). An E-cadherin-mediated hitchhiking mechanism for *C. elegans* germ cell internalization during gastrulation. *Development* **139**, 2547-2556.
- da Graca, L. S., Zimmerman, K. K., Mitchell, M. C., Kozhan-Gorodetska, M., Sekiewicz, K., Morales, Y. and Patterson, G. I.** (2004). DAF-5 is a Ski oncoprotein homolog that functions in a neuronal TGF beta pathway to regulate *C. elegans* dauer development. *Development* **131**, 435-446.
- Dalfo, D., Michaelson, D. and Hubbard, E. J.** (2012). Sensory regulation of the *C. elegans* germline through TGF-beta-dependent signaling in the niche. *Current biology* **22**, 712-719.
- Hutter, H. and Schnabel, R.** (1994). *glp-1* and inductions establishing embryonic axes in *C. elegans*. *Development* **120**, 2051-2064.
- Kamath, R. S., Fraser, A. G., Dong, Y., Poulin, G., Durbin, R., Gotta, M., Kanapin, A., Le Bot, N., Moreno, S., Sohrmann, M., et al.** (2003). Systematic functional analysis of the *Caenorhabditis elegans* genome using RNAi. *Nature* **421**, 231-237.
- Karp, X. and Greenwald, I.** (2003). Post-transcriptional regulation of the E/Daughterless ortholog HLH-2, negative feedback, and birth order bias during the AC/VU decision in *C. elegans*. *Genes & development* **17**, 3100-3111.
- Karp, X. and Greenwald, I.** (2004). Multiple roles for the E/Daughterless ortholog HLH-2 during *C. elegans* gonadogenesis. *Developmental Biology* **272**, 460-469.
- Korta, D. Z., Tuck, S. and Hubbard, E. J.** (2012). S6K links cell fate, cell cycle and nutrient response in *C. elegans* germline stem/progenitor cells. *Development* **139**, 859-870.

- McGovern, M., Voutev, R., Maciejowski, J., Corsi, A. K. and Hubbard, E. J.** (2009). A "latent niche" mechanism for tumor initiation. *Proceedings of the National Academy of Sciences of the United States of America* **106**, 11617-11622.
- Noyes, M. B., Meng, X., Wakabayashi, A., Sinha, S., Brodsky, M. H. and Wolfe, S. A.** (2008). A systematic characterization of factors that regulate Drosophila segmentation via a bacterial one-hybrid system. *Nucleic Acids Res* **36**, 2547-2560.
- Park, D., Estevez, A. and Riddle, D. L.** (2010). Antagonistic Smad transcription factors control the dauer/non-dauer switch in *C. elegans*. *Development* **137**, 477-485.
- Patterson, G. I., Koweeck, A., Wong, A., Liu, Y. and Ruvkun, G.** (1997). The DAF-3 Smad protein antagonizes TGF-beta-related receptor signaling in the *Caenorhabditis elegans* dauer pathway. *Genes & development* **11**, 2679-2690.
- Sijen, T., Fleenor, J., Simmer, F., Thijssen, K. L., Parrish, S., Timmons, L., Plasterk, R. H. and Fire, A.** (2001). On the role of RNA amplification in dsRNA-triggered gene silencing. *Cell* **107**, 465-476.
- Simmer, F., Moorman, C., van der Linden, A. M., Kuijk, E., van den Berghe, P. V., Kamath, R. S., Fraser, A. G., Ahringer, J. and Plasterk, R. H.** (2003). Genome-wide RNAi of *C. elegans* using the hypersensitive rrf-3 strain reveals novel gene functions. *PLoS biology* **1**, E12.
- Simmer, F., Tijsterman, M., Parrish, S., Koushika, S. P., Nonet, M. L., Fire, A., Ahringer, J. and Plasterk, R. H.** (2002). Loss of the putative RNA-directed RNA polymerase RRF-3 makes *C. elegans* hypersensitive to RNAi. *Curr Biol* **12**, 1317-1319.
- Sims, J. R., Ow, M. C., Nishiguchi, M. A., Kim, K., Sengupta, P. and Hall, S. E.** (2016). Developmental programming modulates olfactory behavior in *C. elegans* via endogenous RNAi pathways. *eLife* **5**:e11642.
- Swanson, M. M. and Riddle, D. L.** (1981). Critical periods in the development of the *Caenorhabditis elegans* dauer larva. *Developmental biology* **84**, 27-40.
- Tamai, K. K. and Nishiwaki, K.** (2007). bHLH transcription factors regulate organ morphogenesis via activation of an ADAMTS protease in *C. elegans*. *Developmental biology* **308**, 562-571.

- Timmons, L., Court, D. L. and Fire, A.** (2001). Ingestion of bacterially expressed dsRNAs can produce specific and potent genetic interference in *Caenorhabditis elegans*. *Gene* **263**, 103-112.
- Timmons, L. and Fire, A.** (1998). Specific interference by ingested dsRNA. *Nature* **395**, 854.
- Zhang, X. and Greenwald, I.** (2011). Spatial Regulation of lag-2 Transcription During Vulval Precursor Cell Fate Patterning in *Caenorhabditis elegans*lag-2. *Genetics* **188**, 847-858.

## SUPPLEMENTARY FIGURES

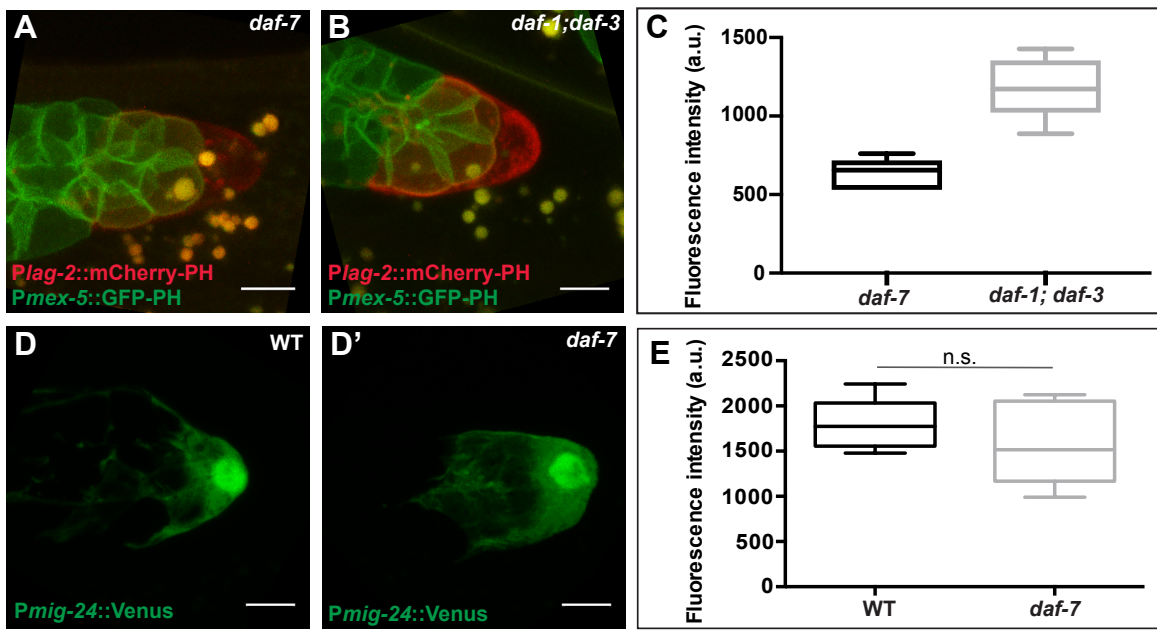


**Figure S1: DAF-7/TGF $\beta$  signaling promotes *lag-2* DTC expression but not *mig-24*.**

(A-C) Expression of *lag-2* (3 kb) reporter *nals37* in distal gonad arms of (A) *daf-7* and (B) *daf-3; daf-1* mutant animals. *naSi1* [*Pmex-5::GFP-PH*] marks germ cell membranes. (C) Quantification of the mCherry signal. (D-E) Comparative expression of *mig-24* promoter in (D) wild type and (D') *daf-7* animals. All images are Z-projections of 0.46  $\mu$ m confocal stacks. Scale bar is 5  $\mu$ m. Mutant alleles: *daf-1(m40)*, *daf-5(e1386)*, *daf-7(e1372)*, *daf-3(e1376)*. (F) Quantification of Venus signal in the DTC. “n.s.” represents “not significant” p>0.05, two-tailed Student’s t-test. N  $\geq$  15 animals; one DTC scored per animal. Error bars represent S.E.M.

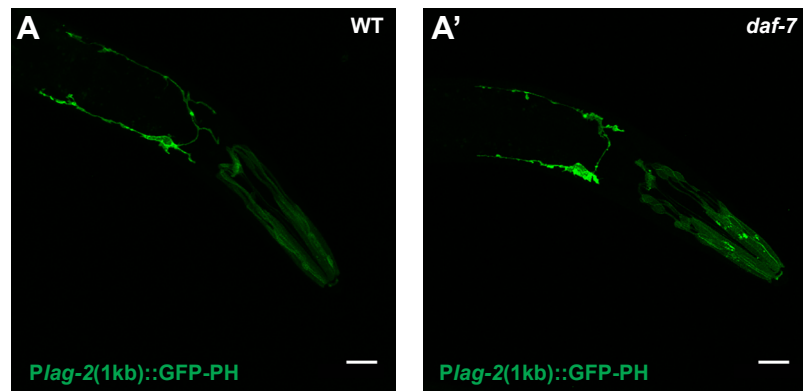


**Figure S2: Neuronal expression of *lag-2* reporter is not changed in *daf-7* animals.**  
Expression of the *nals84* (1 kb) reporter in head neurons of (A) wild type and (B) *daf-7(e1372)* animals. Scale bar is 20  $\mu$ m.

**Plag-2** **TGCGCTGTC**aaaatgtggcaaagattgtgaagtcccctgtagttaacactctaaggta  
ctccaaagacttctacacctgcctacacctgcctatctataaccttagtgccatatcaccta  
ctcgctgcatagttgatgtacctatataacagt**TCATAAAATGAATTGTCAAAATTC**

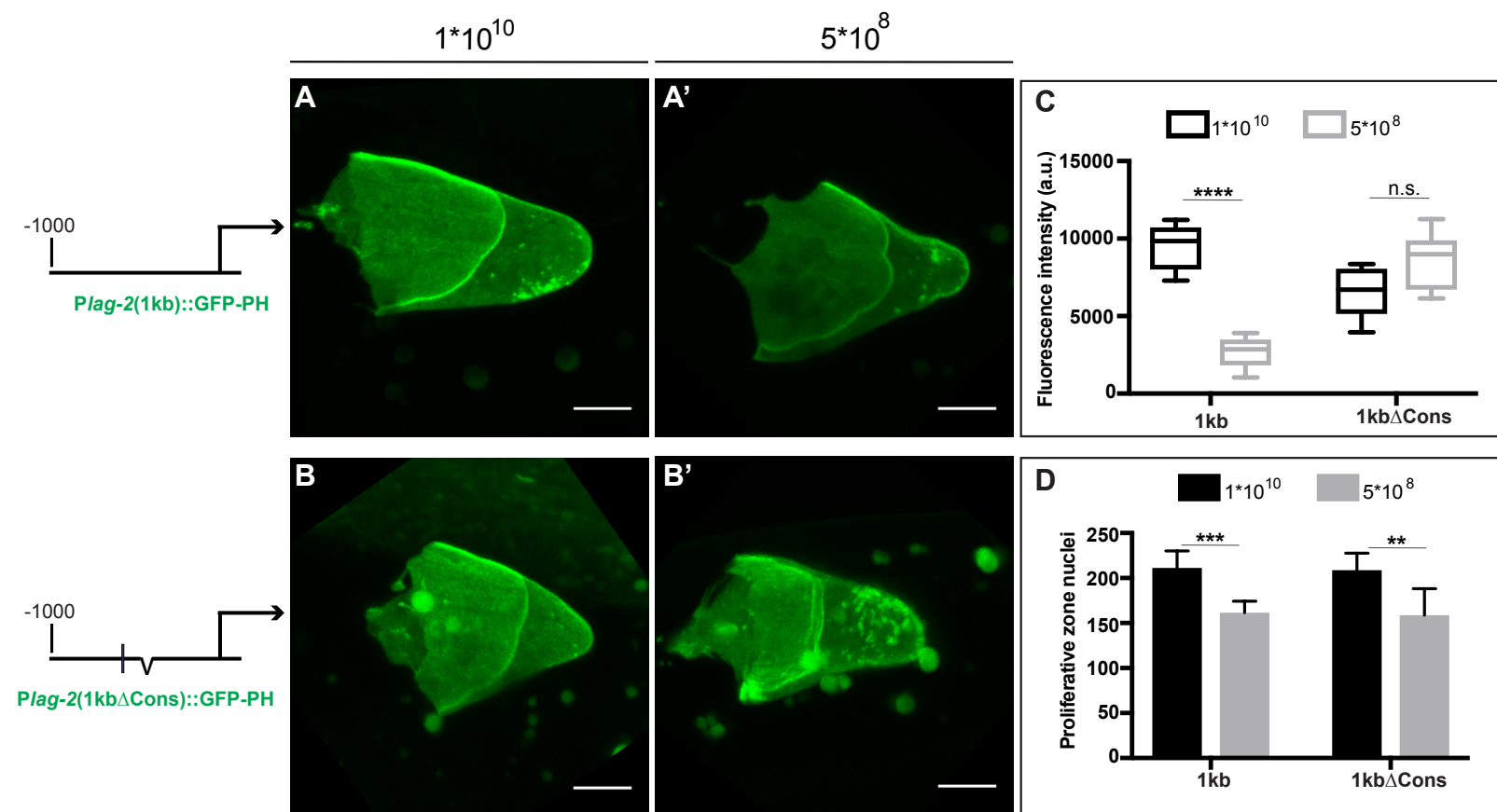
**Posm-9** ctgcgt**GTCTA**tattatcaattttcaccaac**TCTTTAATTTCAGAAACC**

**DBS**    **GTCTG**  
“rule”

**Cons**    **CT [AT] TAA[AT] TTN (0,3) [AC] AN (0,2) TTTTG[CT] CATAA[TA]C[TC]**  
“rule”

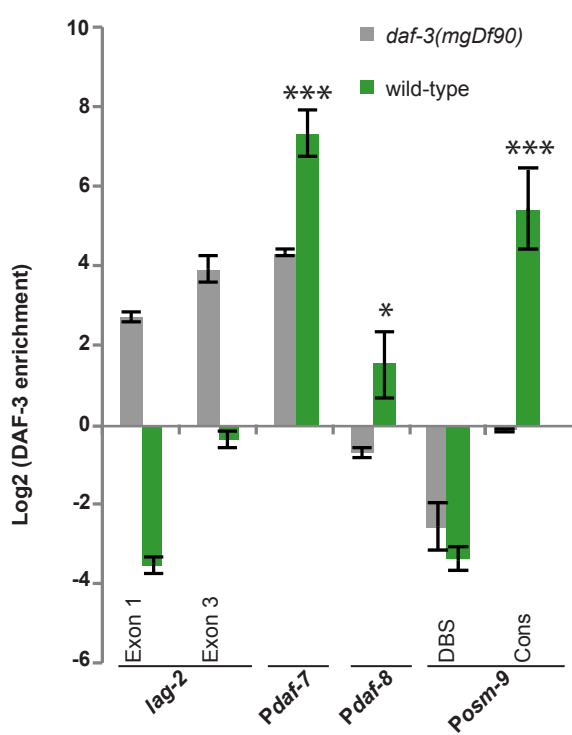
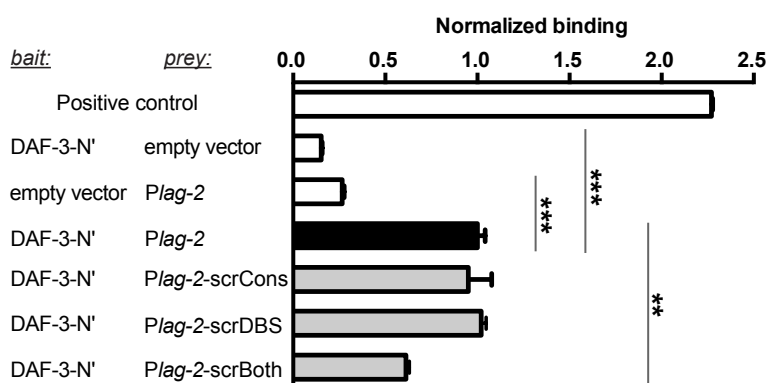
**Figure S3: Related DBS and Cons sequences in the upstream regions of *osm-9* and *lag-2*.**

Sequence in capital letters and in blue and red boxes indicate the DBS and Cons sequences, respectively. Additional related sequence is underlined in *Posm-9*. Bioinformatic analysis identified the related sequences using a flexible version of the depicted “rules” (Sims et al., 2016).



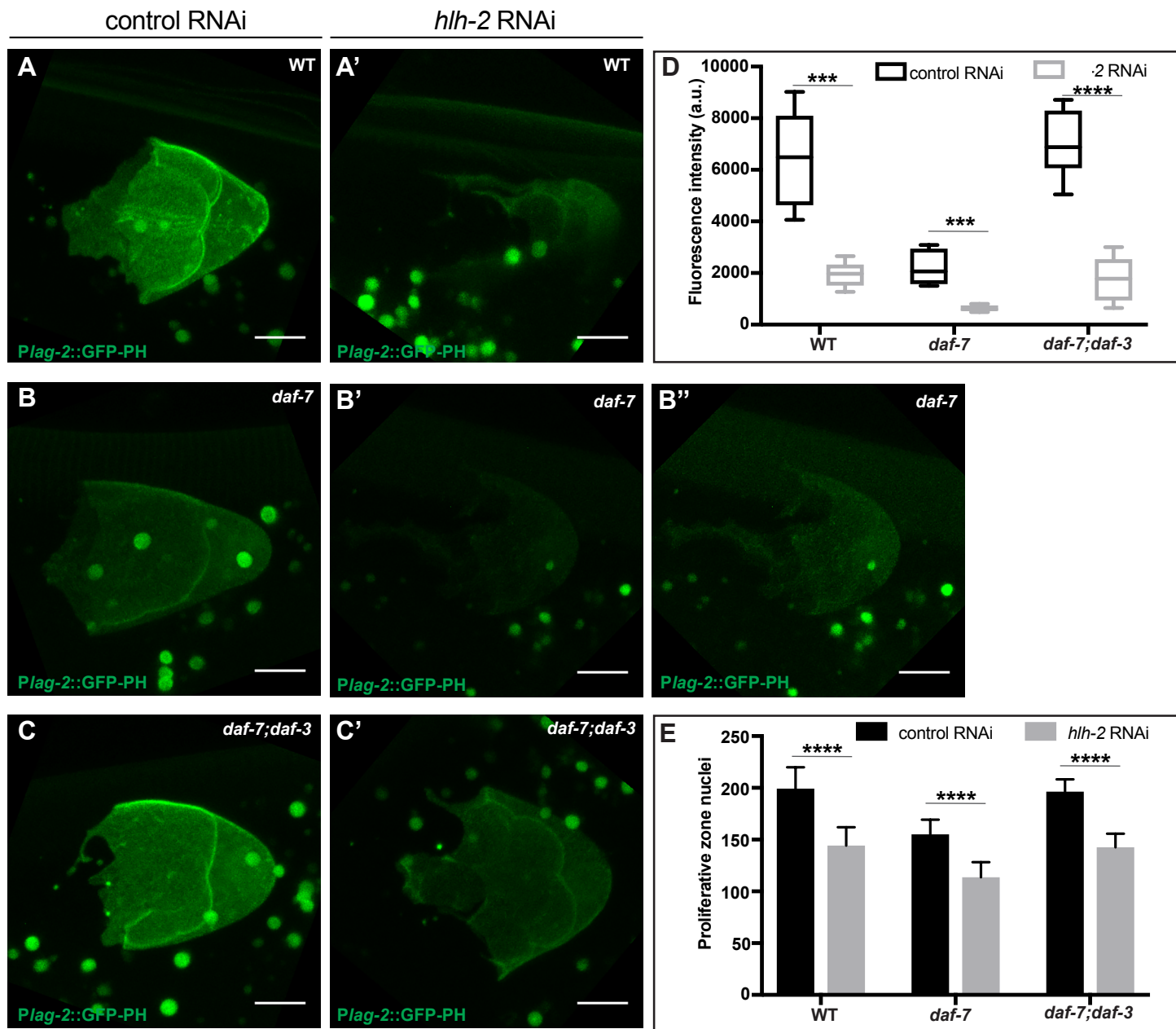
**Figure S4: The Cons sequence is required for *lag-2* reporter response to low food in the DTC.**

(A, B) Representative images of reporter GFP expression driven by 1 kb of the *lag-2* upstream region (*nals84* in strain GC1359) or 1kbΔCons (*nals102* in strain GC1439) in the DTC of late L4 animals reared from early L3 on high ( $1 \times 10^{10}$ ) or low ( $5 \times 10^8$ ) concentrations of OP50 bacteria. All images are Z-projections of 0.46 μm confocal stacks. Scale bar is 5 μm. (C) Quantification of the GFP signal in the DTC from experiments represented in panels A-B. (D) Number of proliferative zone nuclei per gonad arm in early adults (collected from the same plates as animals in previous panels) reared from early L3 on high or low bacterial concentrations. Statistics: “n.s.” is  $p>0.05$ , \*\*\* $p<0.001$ , \*\*\*\* $p<0.0001$ , two-tailed Student’s t-test.  $N \geq 15$  animals, one DTC scored per animal (GFP quantifications) or one gonadal arm per animal (proliferative zone quantifications). Error bars represent S.E.M.

**A****B****Figure S5: DAF-3 binds *lag-2* promoter.**

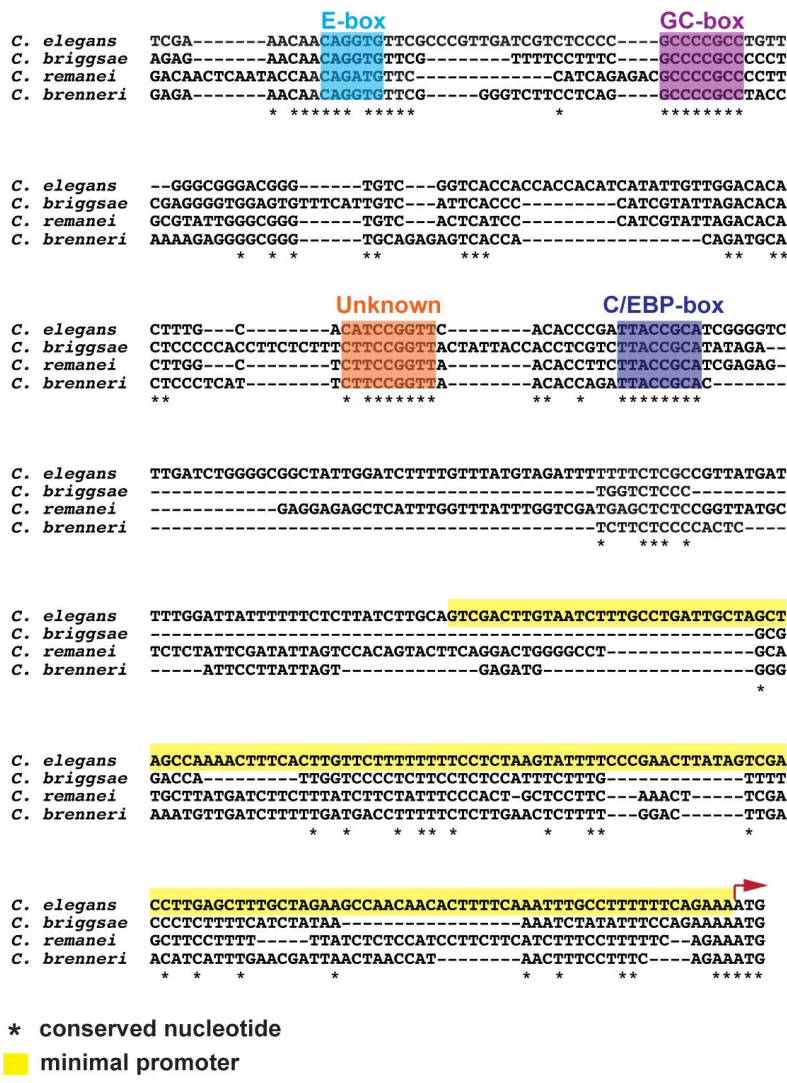
(A) Log2 normalized enrichment of DAF-3 SMAD binding to exons of *lag-2* (as negative controls), to upstream regulatory regions of *daf-7* and *daf-8* (as positive controls), to *osm-9* DBS (as a negative control in animals that have not passed through dauer) and to *osm-9* Cons in wild-type and *daf-3(mgDf90)* strains. Bar graph represents IP-qPCR data, normalized to DAF-3 enrichment at the actin *act-2* promoter (Park et al., 2010). N ≥ 2 biologically independent trials. Significant enrichment in wild-type compared to *daf-3(mgDf90)* is indicated by \*p<0.05, \*\*\*p<0.001, Student's t-test. Error bars represent S.E.M.

(B) Bacterial one-hybrid assay in which N-terminal fragment (up to 250 amino acids, DAF-3-N') of DAF-3 was used as bait and 600 bp upstream of the *lag-2* ATG [*Plag-2(600bp)*] was used as prey. Bar graphs represent FACS analysis data of different baits and preys binding, normalized to DAF-3-N' and *Plag-2(600bp)* (*Plag-2*) binding. Binding of the transcription factor *Zif268* to its consensus target was tested as a strong positive control. Binding of DAF-3-N' to empty prey vector and binding of empty bait vector to *Plag-2* serve as negative controls. Binding of DAF-3-N' to *Plag-2* with scrambled Conserved motif (*Plag-2scrCons*), scrambled DBS motif (*Plag-2scrDBS*) or both (*Plag-2scrBoth*) was tested as well. For sequences of scrambled motifs see Material and Methods. Mean fluorescence for each sample was normalized to the fluorescence of DAF-3-N' paired with the WT *Plag-2* promoter to provide a comparative measure of fluorescence with and without the mutated sequences. \*\*p<0.01, \*\*\*p<0.001, Student's t-test. Error bars represent S.E.M.

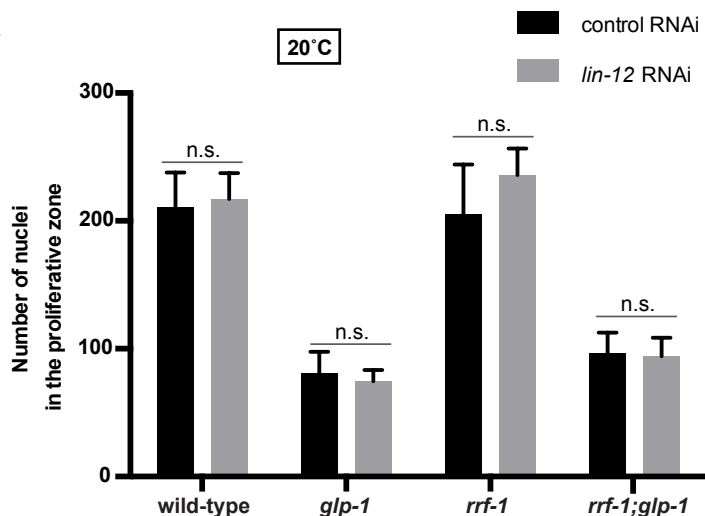
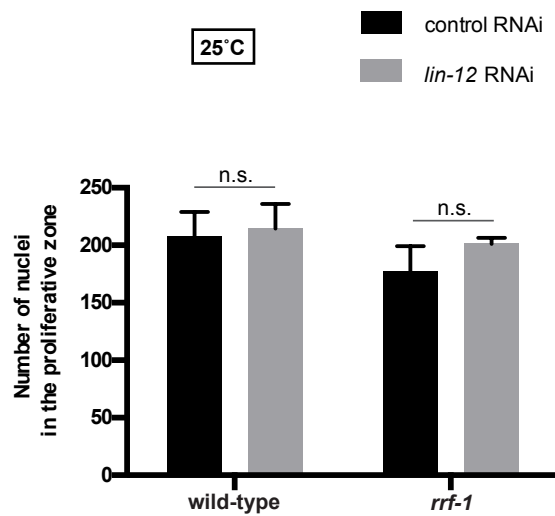
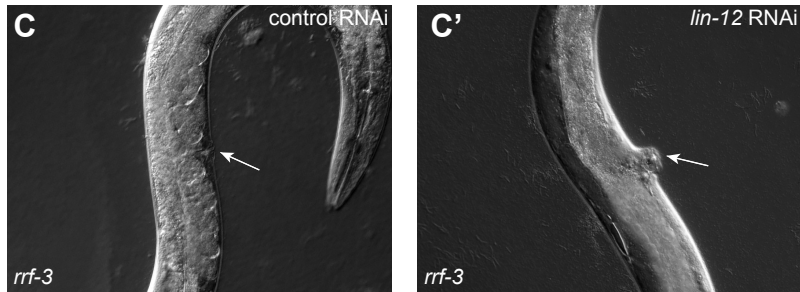


**Figure S6: DAF-7/TGF $\beta$  pathway regulation of *lag-2* DTC expression and germline development occurs in parallel to regulation by HLH-2.**

Expression levels of the *lag-2* single copy reporter (*naSi8*) in (A, A') wild type, (B, B') *daf-7* (B'' is the same image as B' but with enhanced brightness to show residual GFP signal) and (C, C') *daf-7; daf-3* animals treated with control or *hhl-2* RNAi. (D) Quantification of GFP signal in the DTC. (E) Number of nuclei in the proliferative zone of early adults treated with control or *hhl-2* RNAi. All images are Z-projections of 0.46  $\mu$ m confocal stacks. Scale bar is 5  $\mu$ m. Mutant alleles: *daf-7(e1372)*, *daf-3(e1376)*. Statistics: \*\*\*p<0.001 \*\*\*\*p<0.0001, two-tailed Student's t-test. N  $\geq$  15 animals, one DTC scored per animal (GFP quantifications) or one gonadal arm per animal (proliferative zone counts). Error bars represent S.E.M.

**Figure S7: Conserved motifs in the upstream region of *lag-2***

Multiple sequence alignment of ~400 bp upstream of the *lag-2* ATG from different nematode species. Alignment was made using MUSCLE (<http://www.ebi.ac.uk/Tools/msa/muscle/>). The conserved motifs: GC-box/Sp1 binding site and C/EBP-box were identified using MatInspector ([https://www.genomatix.de/online\\_help/help\\_matinspector/matinspector\\_help.html](https://www.genomatix.de/online_help/help_matinspector/matinspector_help.html)). The positions of the E-box/HLH-2 binding site and minimal promoter in *lag-2* promoter are shown as previously reported (Chesney et al., 2009; Karp and Greenwald, 2003; Karp and Greenwald, 2004; Zhang and Greenwald, 2011). We note that the Cons sequence (Fig. S3) is not highly conserved between species, as are these motifs.

**A****B****C****C'**

**Figure S8: Germline-directed LIN-12 RNAi does not affect the number of proliferative germ cells in the early adult.**

(A-B) Number of nuclei in the proliferative zone of early adults (just after the L4/Adult molt) treated with control (L4440) or *lin-12* RNAi at (A) 20°C and (B) 25°C. Mutant alleles were: *glp-1*(e2141), *rrf-1*(pk1417). Animals were fed RNAi-inducing bacteria for two generations: mothers were fed from the first larval stage (L1) and, after transfer to fresh RNAi bacteria, their progeny were scored as adults. The *glp-1*(e2141) mutant at 20°C is a sensitized condition for loss of germline stem cells; reduced TGF $\beta$  signaling dramatically enhances this phenotype (Dalfo et al., 2012). (A) N  $\geq$  12 and (B), N  $\geq$  15 gonad arms. Error bars represent S.E.M; n.s. indicates no significant difference ( $p>0.05$ ) between animals treated with control and *lin-12* RNAi. (C, C') To ensure efficacy of our RNAi reagent, we tested the ability of the same culture of RNAi-inducing bacteria to cause *lin-12* mutant phenotypes. Phenotypes were only observed in the *rrf-3* mutant background that augments somatic RNAi (Simmer et al., 2003; Simmer et al., 2002). Representative images of *rrf-3*(pk1426) animals treated with (C) control or (C') *lin-12* RNAi at 20°C. Normal vulva phenotype in (C) was 100% penetrant (N  $\geq$  100), and disrupted vulva in (C') was 90% penetrant (N  $\geq$  50). Arrows point to vulva.